Addis Ababa University

Addis Ababa Institute of Technology

African Railway Center of Excellence

Design, Modeling, and Analysis of Roof Top Photovoltaic System for Ethio-Djibouti Railway Passenger Trains

A Thesis Submitted to The School of Graduate Studies Of

Addis Ababa University in Partial Fulfillment of The Requirements for The Degree of Masters Of Science In Railway Engineering (Traction And Train Control)

By: Eliyas Dejene

Advisor: **Dr. Ing. Getachew Biru Worku (PhD)**

Addis Ababa Ethiopia
March 2024

Addis Ababa University
Addis Ababa Institute of Technology
African Railway Center of Excellence

Design, Modeling, and Analysis of Roof Top Photovoltaic System for Ethio-Djibouti Railway Passenger Trains

By: Eliyas Dejene

Approved by the Board of Examiners

_____	_____	_____
Chairman, Department Graduate Committee	Signature	Date
Dr.-Ing. Getachew Biru		31.3.2023
Advisor	Signature	Date
Alula Mebratu	_____	_____
Internal Examiner	Signature	Date
Dr.-Ing. Asegid Belay		02/04/2024
External Examiner	Signature	Date

Declaration

I declare that the thesis, titled 'Design, Modeling, and Analysis of Roof Top Photovoltaic System for Ethio-Djibouti Railway Passenger Trains', is my original work. This work is submitted in partial fulfillment of the requirements for the Master of Science degree in Railway Engineering at the Addis Ababa University Institute of Technology, Addis Ababa, Ethiopia. This thesis has not been previously submitted for any other degree or examination in any other institution. All sources of information have been duly cited and acknowledged

Name: Eliyas Dejene Signature: _____

Place: Addis Ababa Institute of Technology, Addis Ababa University, Addis Ababa

Date of Submission: _____

ABSTRACT

The growing demand for electric railway transportation worldwide has led to a rise in power consumption by the transportation system. Hence, providing sufficient, cleaner, and less expensive energy to the transportation system is important to cope with the increasing energy demand. In Ethiopia, the Ethio-Djibouti railway trains consume huge amounts of energy from the national grid for their propulsion and auxiliary services. As the demand for this energy continues to rise, it is crucial to research and explore innovative solutions to meet the increasing energy needs. One potential solution is harnessing solar energy from train rooftops, which can supplement the energy requirements and reduce the stress on the national grid. By adopting this approach, we can alleviate the burden on the grid and enhance the reliability of the power supply.

This research presents a new design and model of a rooftop photovoltaic system for Ethio-Djibouti railway passenger trains. To fulfill the research objective, the solar irradiance function of the train travel schedule across the train route is collected from the European Union weather forecasting web. Following that, the train rooftop PV capacity in contrast with the electrical load demand of the trains was analyzed. Based on the load and PV capacity available, the PV system is optimally sized with an appropriate energy control strategy. Additionally, the PV panels' weight and efficiency are considered during the design phase to improve the practicality and feasibility of the system. Finally, the designed system is modeled and simulated using MATLAB to validate the performance level of the PV system.

The research findings reveal that the designed train rooftop photo-voltaic system can produce up to 393.6 kW. However, energy output is influenced by the train's departure time and location. The designed rooftop PV system can contribute up to 21.318GWh of electric power to Ethio-Djibouti railway passenger trains and yield a net profit of 247,607 USD in its lifetime. Additionally, the return-on-investment value of the PV system is 349%.

***Keywords**: Auxiliary Power Supply System, Photovoltaic and Energy Storage System, Solar train.*

Acknowledgment

I would like to convey my profound appreciation to my mentor, Dr.-Ing. Getachew Biru, whose invaluable counsel, steadfast encouragement, and insightful critiques have been a cornerstone of this research. His knowledge, forbearance, and dedication to high standards have significantly influenced this work.

I would also like to extend my sincere appreciation to all the African Railway Center of Excellence (ARCE) members for providing a conducive learning and research environment. I am grateful for the support I received from the lecturers of the Train and Traction control stream, and I extend my gratitude to Mr. Awol and Dr.-Ing. Assegid for their assistance. I also want to acknowledge my family and friends for their steadfast support, encouragement, and understanding throughout this journey. Their faith in me has been a continuous source of inspiration. I am deeply grateful to the participants of this study who generously gave their time and shared their insights. Without their input, this research would not have been achievable. Lastly, I thank the almighty God, my Father, for His constant presence and guidance throughout this journey. Thank you all for being a part of this incredible journey.

Table of Contents

List of Figure

List of Table

List of Acronyms and Abbreviations

ASAI	Average Service Availability Index
Cdte	Cadmium Telluride.
CIS	Copper Indium Di selenide.
CV	Constant Voltage Method.
CT	Current Transformer.
EC	Ethiopian Calander.
EDR	Ethio-Djibouti Railways.
FLC	Fuzzy Logic Controller.
IC	Incremental Conductance.
I_{pv}	Photo Voltaic Current.
I_{sc}	Short Circuit Current.
kWh	Kilo Watt Hour.
MPPT	Maximum PowerPoint Tracker.
MATLAB	Matrix Laboratory
PV	Photovoltaic.
PVGIS	Photovoltaic Geographical Information System.
ROI	Return on Investment.
STC	Standard Test Conditions.
USD	United States dollar.
V_{pv}	Photo Voltaic Voltage
V_{oc}	Open Circuit Voltage

CHAPTER ONE

INTRODUCTION

Transportation is the backbone of the socioeconomic development of every country in the world. Among the available modes of transportation, electric traction have undeniable benefits in terms of performance, safety, environmental friendliness, and cost-effectiveness. These attributes have led to the increased adoption of electric train transport as a solution to mitigate the congestion and pollution associated with road traffic [1].

With rapid city population development around the world, electric railways are becoming the best choice for transportation, making it necessary that the power supply is reliable and sufficient to provide the demand by electric traction system. Additionally, the need to improve energy efficiency continues to grow, as more capacity is required while electricity costs increase [2], [3].

Therefore, countries have shifted their focus towards harnessing alternative sources of renewable energy to meet the increasing needs of the transportation industry [4]. In contrast to conventional sources, renewable energy emits 750 grams less of CO_2 per kilowatt-hour [5]. Among these sustainable energy options, solar power is widely accessible across various regions globally, particularly in the Middle East and sub-Saharan countries [6]. Therefore, the photovoltaic (PV) power generation sector is regarded as a highly promising field for future advancements.

Ethiopia, an equatorial country in sub-Saharan Africa, benefits from ample sunlight throughout most of its regions. With an average temperature of 28 degrees Celsius and more than 340 to 355 sunny days per year, Ethiopia has the potential to generate 4.5 to 7.3 kilowatt-hours per square meter per day [7], [8]. This abundant solar resource presents an opportunity to utilize this energy for the electrified railway system, such as the Ethio-Djibouti train. By doing so, it would help reduce reliance on non-renewable and hydropower sources while simultaneously decreasing dependency on them. Furthermore, this initiative would contribute to an increase in the overall alternative energy mix level.

Due to the essence of alternative power sources for the growing electrified railway system in Ethiopia, this research investigates how much power can a train rooftop PV system provide for

Ethio- Djibouti railway passenger trains, by considering the effect of the movement of a train on PV power generation.

1.1 Background

The growing demand for electric railway transportation worldwide has led to a rise in power consumption by the transportation system. To maintain the sustainability of electric railway transportation and to cope with the increasing energy demand, it is necessary to provide sufficient, cleaner, and less expensive energy. Therefore, some railway transport providers turn their eyes to exploit alternative renewable energy sources like solar energy.

Solar energy is being used directly either by installing PV modules on the train station and near traction substations or by installing the PV modules on the roof of the train itself. However, solar energy hasn't yet been adopted widely as a direct source of power from rooftops of trains, due to the small installation area and the PV system being an additional load. Interestingly, there have been some recent examples in countries like Australia [9], India [10], and Hungary [11]where solar panels have been installed on train roofs to produce electricity and supply the trains.

In the case of Ethiopia, Ethio-Djiboouti Railway and Addis Ababa Light Rail Transit are the two railway transportation providers in the country. Trains of these operators consume a considerable amount of power from national gird. For example, the Ethio-Djibouti railway train may require up to 7.2 MW of power. Therefore, researches like [4], [12], [13], [14], [15] have been done to reduce stress on the national grid using PV systems.

When developing a rooftop PV system for trains, it is crucial to estimate the potential electric energy production. However, this process is more challenging compared to designing stationary PV systems [16]. This difficulty arises from the fact that the orientation of the PV panels changes as the train moves and the weather conditions vary over long distances. These factors make it difficult to accurately determine the amount of irradiance the panels will receive. Without knowing the exact irradiance, it becomes challenging to determine the specifications of the PV system's components such as the PV panels and converter, and to accurately assess energy production and feasibility. Therefore, when designing rooftop PV systems for trains, it is

important to consider the different weather conditions along the train route instead of relying solely on conventional design procedures meant for stationary PV systems.

Ethio-Djibouti Railway Passenger Trains

Since its commercial launch in January 2018, the Ethio-Djibouti railway has transported almost 530,900 passengers [17] using its fleet of 30-passenger couches. And by the end of 2016 EC, EDR has a plan to double the number of passengers couches it has now. There are four types of couches on the railway:

1. Hard Seat Couch: This couch has a seating capacity of 118 people.
2. Hard Berth Couch: This couch has 66 sleeping beds.
3. Soft Berth Couch: This couch has 36 sleeping beds.
4. Dining passenger couch; This couch is used only for the cafeteria and has 50-person seating capacity.

Ethio-Djibouti railway passenger train uses one locomotive to haul up to 20 passenger couches at a time. The locomotive obtains its power from the national grid through traction substations, which are located near the EDR routes. These traction substations are connected to either the 230kV or 132kV substations of the Ethiopian Electric Power (EEP). The power is then provided to the train through an overhead contact line.

The overhead contact line supplies locomotives with single-phase 25kV AC (50Hz) power. The nominal, maximum, and minimum operating voltages for the overhead catenary system are 25kV, 27.5kV, and 20kV respectively. In abnormal conditions, the maximum and minimum short-time voltages are 29kV and 19kV respectively. The 25kV voltage from the overhead contact line is connected to the main transformer through a pantograph, disconnector, and circuit breaker. The primary winding of the main transformer is connected on one end to the 25kV power source from the pantograph, while the other end is grounded through an axle-end grounding device.

The locomotive's main transformer has 6 secondary windings that produce an output voltage of 3.3kV. These windings are connected to the traction converter. The traction converter uses the 3.3kV output voltage from the main transformer to convert it into DC using a 4-quadrant

converter. This DC voltage is then converted into AC voltage by voltage class IGBT converter components. This AC power is used to supply variable voltage variable frequency (VVVF) power to the 6 traction motors. The main electrical circuit diagram of EDR passenger train locomotive is shown in Appendix I.

In addition to the six secondary windings, the main transformer also has two secondary windings with an output voltage of 860V. These outputs are rectified by converters to provide two independent 600V DC power supplies to all passenger couches connected to the locomotive. Under normal conditions, both 600V DC lines (Circuit I and Circuit II) provide power to the loads. However, if there is a fault in one circuit, it will be automatically disconnected and the other circuit will supply power to the loads. The input end of the 600V DC power supply circuit is equipped with a vacuum contactor, and the output is equipped with an isolating switch that can isolate the input and output as needed. This allows another multi-coupling locomotive power supply device to feed power to the load conveniently.

Inside each passenger couch, the two independent 600V DC supply power AC auxiliary electrical loads such as air conditioners, 220V AC power sockets, refrigerators, water boilers, and stoves through 35kVA inverters. Additionally, the 600V DC is further stepped down to 110V DC to supply various DC auxiliary equipment such as lighting equipment, networking and communication devices, anti-skidding devices, control system equipment, signaling devices, and battery chargers through an 8kW charger controller.

Most of the electrical devices in passenger couches that need an AC power supply require more power to function, whereas most devices that require a DC power supply require less power than the AC load. The main electrical devices of the passenger couches are listed in Appendix II, along with their voltage and power ratings.

Given that the energy output of a photovoltaic (PV) system fluctuates and is not continuous, it is essential to have an effective method for energy storage. There are different types of energy storage systems for different applications. Among the several energy storage systems Ethio-Djibouti railway trains are powered by Nickel-cadmium (NiCd) batteries, which offer several benefits. These batteries are highly durable and resistant to damage. They can be deeply discharged for extended periods without any issues. With proper maintenance, they have a high

cycle count and can be charged quickly with minimal stress. Additionally, NiCd batteries are cost-effective and have a long lifespan with low maintenance requirements. However, it is important to note that they contain the toxic substance cadmium, making them environmentally unfriendly. Another drawback is the presence of memory effect [18]. Despite these limitations, the advantages of NiCd batteries make them ideal for applications like aircraft and electric cars [19].

1.2 Problem Statement

The need for energy in transportation infrastructure is increasing due to the development of countries and global population growth. The Ethio-Djibouti railway trains, like many other electric railway systems, use a large amount of energy sourced totally from the national power grid. In order to address the increasing energy demand and alleviate stress on the national power grid, researchers have investigated ways to reduce power consumption from the grid and utilize alternative sources of renewable energy, such as power derived from the sun generated from the train's rooftop. However, most research in this field relies on conventional methodologies that are only suitable for stationary photovoltaic systems, which overlook the unique characteristics of estimating energy generation capacity for a train rooftop PV system. Treating the train rooftop PV system as a stationary PV system can provide misleading information about its power generation capacity, affecting the practicality and feasibility of the PV system. Therefore, addressing this issue will result in practical benefits when designing and modeling train rooftop PV systems. This research addresses the problem by utilizing hourly irradiance data along the route to calculate energy production for each location and hour, taking into account the impact of the moving train on PV energy generation.

1.3 Research Questions

1. How much potential solar radiation is available on the Ethio-Djibouti route to be used for the PV system?
2. How to consider the effect of the movement of a train on PV power generation?
3. How to efficiently use the energy produced from the PV system?

4. Is a train rooftop PV system feasible?

1.4 Objectives

1.4.1 General Objective

The general objective of this research is to design, model, and analyze a rooftop photovoltaic system to supply auxiliary electrical loads of Ethio-Djibouti passenger trains.

1.4.2 Specific Objectives

The specific objectives of this study are

- To analyze the potential of electric energy generation using a rooftop PV system on the train.
- To analyze the effect of train movement on the energy production of a rooftop PV system.
- Design a reliable and efficient rooftop photovoltaic system for the onboard auxiliary loads in the case of Ethio-Djibouti railway trains.
- To study the feasibility of the train rooftop PV system.
- To evaluate the performance of the designed system, and to draw relevant conclusions and recommendations for future implementation.

1.5 Significance of the Study

The main significance of this research is to inform the Ethio-Djibouti Railways (EDR) about the viability of utilizing renewable energy sources like solar power to power auxiliary loads with renewable energy sources, such as solar power. This can increase the potential use of alternative energy sources and contribute to the country's overall energy mix.

Additionally, the study provides valuable information on how to estimate the potential of train rooftop PV system and suggests ways of harnessing it effectively. This can help save energy cost, reduce reliance on conventional energy sources, and improve power reliability.

1.6 Scope

The scope of this research is to design, model, and analyze a rooftop photovoltaic system that supplies auxiliary electrical loads of Ethio-Djibouti passenger trains. This research does not model the impact of the PV system on the train's traction power system.

1.7 Limitation

Due to the low budget, this study does not measure irradiance and temperature data throughout the Ethio-Djibouti railway route instead it collects satellite irradiance data from selected stations that represent the different geophysical locations of the route. The MATLAB/Simulink environment has been used to model and simulate the entire PV system.

1.8 Thesis Organization

This thesis work is organized into five chapters

Chapter 1: Provides a concise introduction that explains the motivation and purpose of the research. Additionally, it highlights the importance of the research and states the objectives to be achieved.

Chapter 2: Presents a literature review on the background of PV, MPPT algorithm techniques, and related works are discussed.

Chapter 3: Presents the methodology used, solar energy potential assessment through the Ethio-Djibouti railway line, PV system modeling, and detailed design of the PV sub-system and energy management sub-system.

Chapter 4: Summarizes the results and discussion of the simulation done. It also presents the economic analysis of the train rooftop PV system.

Chapter 5: Finally, the conclusion and recommendations made are presented.

CHAPTER TWO

THEORETICAL BACKGROUND & LITERATURE REVIEW

2.1 Introduction

Recently, many studies in [20] have focused on providing sufficient, cleaner, and less expensive energy for the increasing power supply demand of railway transportation. Some railway operators in certain countries have opted to equip their trains with solar photovoltaic (SPV) systems due to the benefits of PV technology. For instance, in Italy, amorphous silicon modules were added to various passenger and freight couches [20]. In Hungary, a solar railcar was developed at the Kismaros workshop, featuring a set of photovoltaic panels covering about 9.9m² on the roof. These panels charge batteries located beneath the seats, supplemented by a regenerative braking system [11]. Indian Railways also joined this trend by installing 1 kWp capacity SPV modules on trains at Pathankot, Punjab, India in 2011, powering electrical loads ranging from LED bulbs to other equipment [21].

Although numerous studies have been conducted on generating electricity using train rooftop photovoltaic (PV) systems to provide the growing power supply demand of railway transportation, only a small number of researchers have considered the influence of train movement on estimating the power generation capacity of the PV system [22].

2.2 Over View of Solar Resources in Ethiopia

Numerous researchers have investigated the solar energy potential in various regions of Ethiopia and have determined that the country receives sufficient solar radiation to support the installation and operation of solar power plants [23]- [26].. For example, Frances Drake and Yacob Mulugeta [23] used empirical models to predict solar radiation based on sunshine hours. They observed a linear and quadratic correlation between monthly mean daily solar radiation and daily sunshine hours across seven stations in Ethiopia, demonstrating that solar energy is abundant across all regions.

N. Argaw [24] focused on estimating solar radiation levels in different locations in Ethiopia, such as Addis Ababa, Bahir Dar, Nedjo, and Zeway, with recorded values ranging from 4.13 kW/m2/day to 6.62 kW/m2/day using Angstrom regression models based on sun hour data.

Fikremariam Teshome's [25] research on solar energy resources in Ethiopia revealed a solar radiation potential ranging from 0.2 MWh/m^2/year in the lowlands to 2.6 MWh/m^2/year in the central highlands. By analyzing topographic, economic, and environmental factors, Teshome identified 195 sites predominantly in the eastern region covering 6000 square kilometers as ideal locations for large-scale photovoltaic installations. If harnessed effectively, these sites could potentially generate more than 65 Giga Watt assuming a 10 percent photovoltaic efficiency.

The Ethiopian resource group reports that [26] Ethiopia receives between 5.5 to 6.5 kilowatt-hours per square meter per day of solar insolation for more than an average of 345 days a year. Solar energy availability remains relatively stable throughout the year in lowland regions (less than 10% deviation from the average) but shows significant variation in highland areas (more than a 25% deviation from the average). Consequently, Ethiopia possesses significant potential to harness more energy from sunlight

2.3 Photovoltaic Technologies

A photovoltaic panel is a device that converts solar radiation into electrical energy through the photovoltaic effect. There are different types of photovoltaic panels that vary with their production process, production material, conversion efficiency, and physical properties, some of the most known are listed below.

a. Monocrystalline Silicon Solar Panels: These panels are made from cells cut from a single silicon crystal, offering high efficiency of around 22-24%. However, their slow and labor-intensive production process leads to slightly higher costs compared to other solar technologies. Recent advancements have reduced the amount of silicon material used in these cells to lower costs.[27]

b. Polycrystalline Silicon Solar Panels: These panels contain multiple small crystal grains, making them cheaper to produce than monocrystalline panels and less efficient than monocrystalline silicon solar cells with and average efficiency of 12% [28].

c. Amorphous Silicon (Thin-film) Solar Panels These panels are slim, flexible, and made by applying a silicon film onto a glass base. They use fewer resources and energy to manufacture than crystalline cells, which makes them more affordable but less efficient.

e. Cadmium Telluride (CdTe) solar panel CdTe panels are a type of thin-film solar panel that are more efficient than amorphous silicon panels. However, there are worries about the limited supply of tellurium and the potential harmful effects during disposal due to the presence of cadmium. [29].

f. Copper Indium Gallium Selenide (CIGS) **solar panel -** CIGS cells are created by depositing a thin film on a base and have good resistance to heat. They are one of the most efficient thin-film photovoltaic technologies with an efficiency close to 20% and do not contain harmful cadmium. However, despite promising laboratory results, mass production of CIGS cells has proven to be difficult.

PV technologies with higher efficiency, like gallium arsenide and multi-junction cells, are also employed in the making of PV panels. However, their usage is not widespread due to their expensive nature, but they are perfectly suited for concentrated photovoltaic systems and applications in space.

Each type of PV technology is preferred in different application areas depending on the properties they have. Monocrystalline silicon cells are ideal for situations where high efficiency is needed, and where there is limited installation area. Polycrystalline silicon cells are suitable for large-scale solar farms because they are less expensive. Thin film cells are useful for building integrated photovoltaics or portable applications due to their flexibility and less weight. Higher efficiency technologies are used in concentrated photovoltaic systems or space applications.

The electrical response of a solar cell is represented using a model based on a p-n junction with nonlinear characteristics. Researchers employ various models to describe photovoltaic (PV)

cells, with the simplest equivalent circuit being a current source in parallel with a diode. [30] as shown in Figure 2.1.

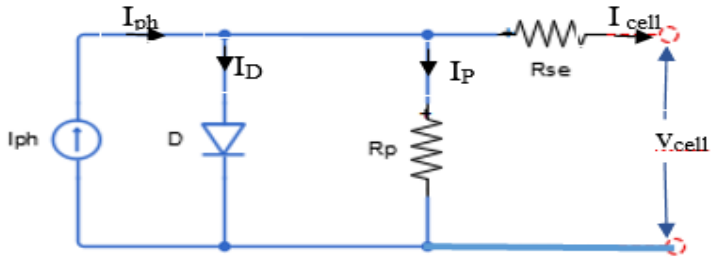

Figure 2.1 Equivalent Circuit Diagram of a Solar Cell [30].

This model assumes that the solar cell acts like a current source proportional to incident light, behaving as a diode in illuminated conditions and being inactive in darkness. The cell's I-V characteristics are determined by the diode 'D'. The equivalent circuit includes a shunt resistor 'R_p' for junction leakage current and serial resistors 'R_{se}' for contact and connection resistance.

The output current 'I_{cell}' from the cell is calculated using Eq. 2.1, where 'I_D' is diode current, 'I_{Rp}' is shunt resistor current, and 'I_{ph}' is photocurrent influenced by solar irradiation and temperature, calculated by Eq. 2.2. In this equation, 'K_t' is the Temperature coefficient of the short circuit, 'G' is irradiance, 'G_{ref}' is reference irradiance, 'T_c' is cell temperature, and 'T_{ref}' is nominal temperature at 25°C. [23]– [25].

$$I_{cell} = I_{ph} + I_D + I_{Rp} \tag{2.1}$$

$$I_{ph} = \frac{G}{G_{ref}}(I_{phref} + K_t(T_C + T_{ref}) \tag{2.2}$$

The diode current 'I_D' is given by Eq. 2.3, which illustrates the nonlinear behavior of the semiconductor diode using the reverse saturation current 'I_s', which is variable with temperature Boltzmann constant 'k', ideality factor 'n', temperature 'T_C', and diode voltage 'V_d'. Since the parallel load voltage is constant, Vd = VRp, and the shunt current 'IRp' can be expressed using Eq. 2.4.

$$I_d = I_s e^{\left(q\frac{V_d}{nkT_c} - 1\right)} \tag{2.3}$$

$$V_d = I \times R_P = V_c + R_{se} \times I_{cell} \tag{2.4}$$

Based on the previous equations, the expression of the panel current can be expressed in Eq 2.9

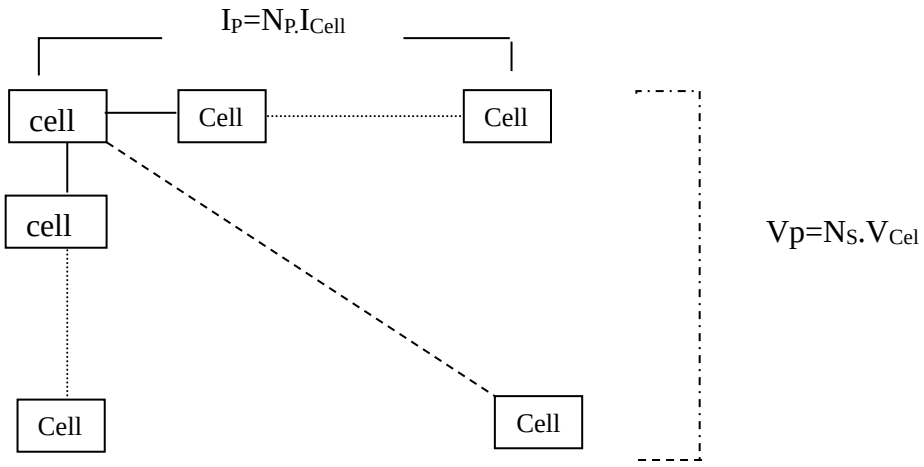

Figure 2.2 Equivalent Model of Photovoltaic Cells into a Panel

$$I_{cell} = \frac{I_P}{N_P} \tag{2.5}$$

$$V_{cell} = \frac{IV_P}{N_S} \tag{2.6}$$

$$V_d = \frac{V_p}{N_S} + \frac{R_{se} \times I_p}{N_p} \tag{2.7}$$

$$I_{Rp} = \frac{1}{R_p}\left(\frac{V_p}{N_s} + \frac{R_{se} \times I_p}{N_P}\right) \tag{2.8}$$

Panel current (I_p)= $N_P I_{PH} - N_P I_S \left(e^{\frac{q}{nKTc}\left(\frac{Vp}{Ns}+\frac{Rse.Ip}{Np}\right)-1}\right) - \frac{Np}{Rp}\left(\frac{Vp}{Ns} + \frac{Rse.Ip}{Np}\right)$ (2.9)

Table 2.1 Ideality Factor [34]

Technology	**Ideality factor**
Si-mono	**1.2**
Si-poly	**1.3**
a-Si-H	**1.8**
CdTe	**1.5**
CTs	**1.5**
AsGa	**1.3**

2.4 Factors Affecting PV System Performance

Researches [35], [36], [37], [38], [39] show performance of PV system are influenced by many factors, such as irradiance of the location, cell operating temperature, shading or partial shading, and array orientation.

Irradiance

The amount of solar power per unit area that is received from the sun in the form of electromagnetic radiation is called irradiance. Irradiance is measured in watts per square meter (W/m^2). The energy generated by a photovoltaic module is directly proportional to the amount of solar irradiance available, which is dependent on the location of the site [40]. The total irradiance on a PV panel determines the output power of the PV panel. When the amount of irradiance on a PV panel increases the output power by the panel also increases or vice-versal. Irradiance level is affected by the sunny hour in the day, passing clouds, hazy weather, and air pollution. With a constant temperature, an increase in irradiance leads to a rise in both the short-circuit current and the open-circuit voltage [36].

Temperature

The performance of a photovoltaic (PV) panel is influenced by temperature changes, affecting its power output, current, and voltage [41][35]. Specifically, as the temperature rises, the open circuit voltage decreases significantly while the short-circuit current increases only slightly, leading to a decrease in overall output power. Researches [28], and [34], emphasizes the importance of distinguishing between ambient temperature and module temperature, with findings indicating that module temperature has a greater impact on PV output power.

Shading

Shading can be caused by various obstructions near PV arrays that reduce or block sunlight on PV arrays, such as trees, buildings, accumulated soiling on the panels and even other parts of the array itself. Since PV cells in a PV module are connected in series and thus all the cells have the same current, if one of them is shaded the current output of it will be reduced so does the total output current. Shading also causes the formation of different local maxima[42] which makes

difficult MPP tracking. Generally, shading reduces the amount of power produced by PV arrays, since it reduces the amount of irradiance on PV arrays[43].

Wind Velocity

Wind may serve as a natural coolant [44]. The temperature of solar panels decreases with wind speed. A sufficient wind speed can also assist in removing dust that has settled on the panels. This leads to an increase in the module's efficiency due to the reduction in temperature and dust removal. However, extremely low or high wind speeds do not contribute to power output enhancement. The module's performance is impacted by factors beyond just wind speed; it is also influenced by wind direction and elevation. A study [36] examines how changes in wind speed affect the electrical efficiency of the PV module. Furthermore, it demonstrates that the highest power output, efficiency, and fill factor are achieved at a wind speed of 33.26 m/sec.

Array Orientation

The position and angle of a system affect how much sunlight it can capture [40]. Maximum energy can be collected when the array is perpendicular to the sun. The orientation of photovoltaic arrays is determined by two angles known as azimuth and tilt angles. The azimuth angle signifies the direction in which an array is facing with respect to compass headings or relative to due south. North is 0^o or 360^o, east is 90^o, south is 180^o and west is 270^o. The general rule states that in the northern hemisphere, the ideal azimuth angle is towards due south, while in the southern hemisphere, it is due north [45].. The tilt angle is the angle between the array surface and the horizontal plane. The optimal relationship between tilt angle and latitude serves as a guideline for estimating the best tilt angle for different locations. However, this approach may not always provide the most accurate values [47]. Therefore, using solar radiation data particular to a location is crucial to determine the precise optimal tilt angle for that specific area.

Generally, these factors affecting the energy output of a photovoltaic (PV) system are interdependent. For instance, the orientation of the PV array affects the amount of irradiance that a PV panel receives, and the irradiance itself can affect the temperature of the PV panels. Wind speed and direction can also affect the temperature of the panels. Even though they all affect the energy output of the system their impact is not equal as shown in research [48]. According to

research [48], irradiance has a higher impact on the energy output than other factors. For instance, in the case of train rooftop PV systems for EDR, the cooling effect of wind will compensate for the impact of temperature, and the impact of shading will be minimal since the route is mostly rural with no big trees. The wind will also sweep off the dust, ensuring that the panels remain clean and efficient

2.5 Photovoltaic Maximum Power Point Tracking Systems

Converting solar energy into electrical energy presents significant challenges. Firstly, solar photovoltaic (PV) cells exhibit relatively low efficiency, particularly in areas with limited sunlight. Secondly, the electricity output from solar PV panels is inconsistent due to changing atmospheric conditions. Another issue is that the current-voltage (I-V) curve of a solar cell is nonlinear and fluctuates depending on sunlight intensity and temperature. The I-V or power-voltage (P-V) curve typically has a Maximum Power Point (MPP), where the solar PV system achieves peak power output.

To address these efficiency limitations, various methods have been developed for monitoring and maximizing the power output of a Photovoltaic module [14], [49], [50].. One such method is the Maximum Power Point Tracking (MPPT) system, which optimizes the power transfer from the solar PV panel to the load. It functions as a DC-to-DC converter, ensuring that the solar arrays operate efficiently with the load by continuously adjusting the operating parameters of the PV modules to extract the maximum available power. Some of the widely used MPPTs are described below.

Constant voltage method (CV)

The constant voltage [51] method in photovoltaic systems is used to keep the bus voltage stable by adjusting the duty cycle of the DC-DC converter based on the comparison between the PV system output voltage and a reference voltage to track the Maximum Power Point (MPP). While simple and cost-effective with only one feedback loop control, this method cannot effectively adapt to environmental variations like temperature or irradiation changes.

Perturb and observe the algorithm

The Perturb and Observe (P&O) algorithm involves adjusting the operating voltage of the PV array to find the MPP. If increasing the voltage leads to a power increase, it indicates that the MPP is to the right of the current point and further voltage adjustment to the right is needed. Conversely, if a voltage increment results in lower power, the MPP is likely to the left, requiring adjustments in that direction. Although this method guides towards the MPP, it tends to oscillate around it rather than precisely reaching it [52]. To mitigate oscillations, reducing the perturbation step size can help but may impact overall tracking performance. Limitations include its inability to efficiently handle changing irradiance and temperature conditions impacting the PV array.

Incremental conductance algorithm

The incremental conductance (IC) technique was developed to address oscillation issues resulting from various iterative methods [53]. It boasts superior performance in rapidly changing weather conditions and exhibits reduced oscillations around the Maximum Power Point when compared to the P&O technique. Nevertheless, a drawback of this approach is its inability to achieve the zero-point condition, which results in some power loss.

The basis of the incremental conductance method is the observation that the power versus voltage curve of a PV module has a slope of zero at the MPP, positive to the left, and negative to the right. The PV operating point relative to the MPP can be determined using conductance (I/V) and incremental conductance (dI/dV). When

$$\frac{dV}{dP} = 0, \text{ at the MPP,}$$

$$\frac{dV}{dP} > 0, \text{ on the left,} \qquad (2.10)$$

$$\frac{dV}{dP} < 0, \text{ on the right.}$$

$$\text{And } \frac{dp}{dv} = \frac{d(IV)}{dv} = I + V\frac{dI}{dV}$$

Eq. (2.10) can be rewritten as

$$\frac{dI}{dV} = -\frac{I}{V}, at\ MPP$$

$$\frac{dI}{dV} > -\frac{I}{V}, at\ Left\ of\ MPP$$

$$\frac{dI}{dV} < -\frac{I}{V}, at\ Rigth\ of\ MPP$$

When dV/dP equals zero at the MPP, it indicates the optimal operating point, while dV/dP greater than zero signifies the left side of the MPP, and less than zero indicates the right side. Additionally, the equation dp/dv=(d(IV))/dv=I+V dI/dV signifies the relationship between power, current, and voltage. To track the MPP during changes in solar irradiance, adjustments to the operating voltage of the PV module are made accordingly – increasing voltage when irradiance rises and decreasing it when irradiance falls. The MPP can be pinpointed by utilizing the incremental conductance method. If the incremental conductance matches the negative of the instantaneous conductance, the PV module is at the MPP. Conversely, if the incremental conductance exceeds the negative of the instantaneous conductance, adjustments should increase the operating voltage to the left of the MPP, and vice versa for the right side of the MPP.

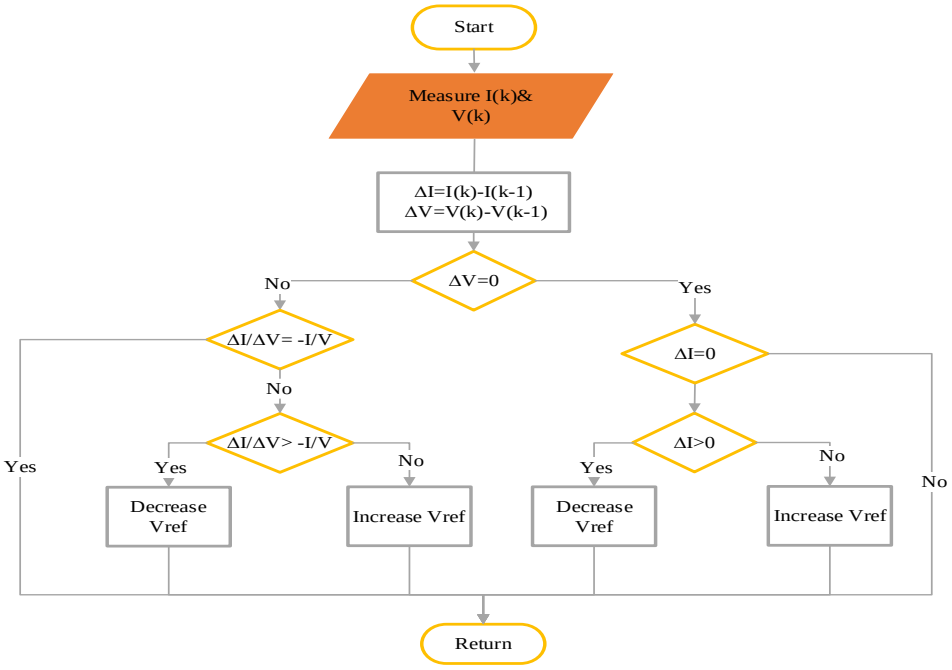

Figure 2. 3 Incremental Conductance MPPT Algorithm Flowchart

Fractional open-circuit voltage

Fractional open-circuit voltage refers to the relationship between the maximum power point voltage (VMPP) and the open circuit voltage (VOC) of a photovoltaic array, exhibiting a near-linear correlation across changing temperature and irradiance conditions. This results in a fractional open circuit voltage, which is typically measured by briefly disabling the converter, although this method has drawbacks such as temporary power loss during shutdown. Recent research efforts aim to address these limitations [54].

Fractional short circuit current

The fractional short circuit current technique is based on the concept that the current at the maximum power point of a solar panel module is closely linked to the short circuit current under different atmospheric situations. This method requires an additional switch to be incorporated parallelly with the PV module to gauge the short circuit current of the PV system effectively. [14].

Fuzzy Logic Control

Fuzzy logic control (FLC) based Maximum Power Point Tracking (MPPT) algorithm is an intelligent strategy that leverages human expertise rather than relying solely on the system's mathematical model to identify and maintain the optimal operating power point of a PV system [55]. FLC offers advantages like handling imprecise input data, not mandating an exact mathematical model, and addressing nonlinearity issues. However, the user's knowledge plays a crucial role in determining the efficiency of the MPPT process. The Fuzzy Logic Control comprises three key stages: Fuzzification, Inference System employing Madani's table method, and Defuzzification to calculate the output (duty cycle) using the center of gravity [56].

The fuzzy logic control (FLC) based MPPT algorithm is an intelligent technique that tracks the maximum operating power point of a PV system. It relies on human experience rather than the system’s mathematical model [55]. This technique has several advantages such as handling imprecise input, not requiring a precise mathematical model, and management of nonlinearity. However, user knowledge is very essential factor that determines the efficiency of the MPP. The FLC is made up of three stages: Fuzzification, Inference System (which involves looking up

rules in a table), and Defuzzification. Fuzzification involves converting numerical inputs into linguistic variables based on their membership to specific sets. The Inference System is implemented using Madani's table method, and Defuzzification calculates the output of the FLC (the duty cycle) using the center of gravity [56].

Various researchers have compared numerous MPPT algorithms based on factors such as application suitability, implementation complexity, ability to track the actual Maximum Power Point (MPP), and cost-effectiveness [14], [49], [56], [57]. Their analysis provides electricity companies and researchers with insights to select the most suitable MPPT technique for a solar energy system based on effectiveness and economic viability, aiding in making informed decisions regarding MPPT algorithm choices.

For rooftop PV systems most research done [12], [13], [24], [25] simply selected the popular P&O MPPT algorithm. However, research [58] presented a detailed analysis of different MPPT techniques based on factors such as the method’s implementation, its capability to accurately track the true MPP, and installation cost for the application of a rooftop PV system. The research simulated and compared the potential of the PV system using the actual situation in Ethiopia and finally showed that the incremental conductance MPPT method is superior for the case of Ethiopia.

2.6 Solar Energy in Railway

The utilization of solar energy in railway systems is currently constrained by the absence of advanced technologies. However, certain countries are contemplating implementing this system for various purposes in their railway networks. Researches are also being done focusing on expanding the application of photovoltaic systems in railways.

M. S. Vasisht, G. A. Vashista, et al [33] conducted a study on the viability of a rooftop solar photovoltaic system on railway couch. Their findings indicated that a single rail couch can produce a minimum of 18 kWh of electricity per day, leading to savings of 1700 liters of diesel annually and a reduction of 45 tons of carbon dioxide emissions per carriage per year.

Wang Wei et al [32] proposed an auxiliary power supply system for passenger trains in China, incorporating photovoltaic panels and energy storage. The paper describes the system's structure, photovoltaic panel installation methods, Maximum Power Point Tracking (MPPT) algorithm, stability control strategy, and energy management strategy. It also provides an estimated annual power generation capacity, analyzes system efficiency, energy conservation impact, and emissions reduction. The MPPT algorithm employed in this system is perturb and observe.

Mitiku Tilahun [4] studied the technical feasibility and design of a grid-connected PV system for the Ethio-Djibouti railway line. This research will reduce dependency on one type of energy source (hydropower plant). But these systems are costly, and still vulnerable to transmission losses and if there is any fault on a transmission line, a train will not have any other option other than using their backup storage, which will not last long. This may cause loose of communication with the operation control center, essential data, and interruption of a train. Therefore, an onboard photovoltaic and energy storage system is preferable to avoid the previously stated problems.

Shimels, K. [13] studied the daily and monthly amount of solar radiation through Ethio-Djibouti railway routes and calculated electrical energy that can be harvested from train rooftop PV systems through AALRT and Ethio-Djibouti routes. This research also predicts that the energy produced by the PV system may cover 4.45 to 356.90% of the demand energy based on the irradiance received, types of cars, and configuration. However, the first mistake made by this research is considering the power consumption of Ethio-Djibouti railway trains as 815.4 KW, where the exact maximum consumption is about 7.2 MW. The other limitation of this research is, not considering any hourly irradiance change, since the train travels a long distance there is a difference in irradiance. Due to this, the estimated power and energy production of the system is exaggerated. Lastly, the effect of the movement of the train on PV energy production and the effect of the mass of PV panels is not discussed in this research.

Regis Nibaruta [12] proposes a strategy for an onboard auxiliary supply system of AALRT using photovoltaic and battery energy storage. This research calculated the yearly average irradiance in Addis Ababa city and estimated the power production of the system.

Most of the research [12], [13], [14], [32], [33] stated above does not consider the effect of the movement of the train, for a moving train irradiance and temperature on the rooftop of the train varies with the speed and the position of the train. Therefore, this study considers hourly irradiance for each position of the train instead of using the average value irradiance of the whole route to calculate the PV system's generation capacity.

CHAPTER THREE

Design and Modeling

In this research section, the first part presents the various methodological approaches and procedures employed to gather solar radiation data. Following that, it examines the potential for electric energy generation utilizing the train's rooftop and conducts a load analysis. Lastly, it delves into the process of designing and modeling a rooftop photovoltaic (PV) system.

3.1 Data Collection and Analysis

3.1.1 Methodology

To provide increasing energy demand and reduce the amount of electricity that has to be provided by the national power grid, many researches have been done which reduce power usage from the national power grid and increase the exploitation of alternative renewable energy sources like train rooftop solar energy. Even though there is an increasing demand for high-quality energy output prediction, most of these researches follow the conventional methodology, which applies only to stationary PV systems, in designing and modeling the system. Thus, in this research hourly irradiance of sites where the trains arrive is considered instead of simply taking an average value of the whole route, and also the effect of PV system weight and efficiency were considered in the designing part to improve the practicability of the PV system.

Therefore, to model and design an efficient rooftop PV system many literature papers were reviewed, and the limitations of the previously done research were identified. Then the required data about passenger couches load requirement and the route of EDR was collected from Ethio-Djibouti railway SC and the solar irradiance on the rooftop of a train at various times, azimuth, slope, and locations on the route was collected from the EU science hub database (PVGIS) [59], which is validated by [60], [61], [62], [63]. After the data collection and calculations were done train rooftop PV system with battery backup for EDR was designed. The designing included sizing and selecting the PV panel and battery and designing the power and control circuit of the system. The designed system is modeled and simulated using MATLAB to validate the designed calculation outputs. Finally, the design calculation and model simulation results were analyzed for various departure times and departure locations, and the findings were subsequently

presented.

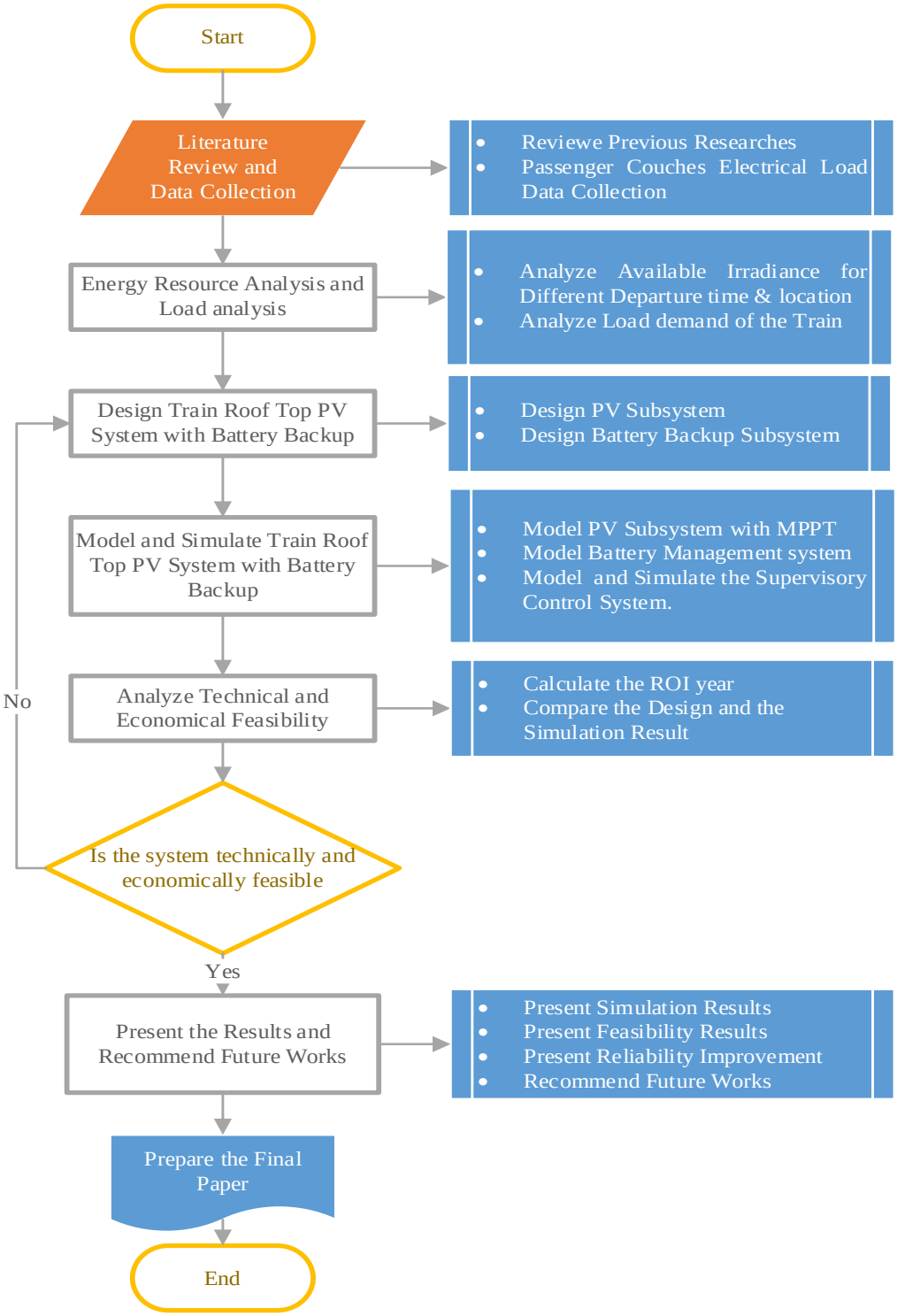

Figure 3. 1 Flow Diagram Showing the Methodology

3.1.2 Solar Energy Assessment for Ethio-Djibouti Railway Route.

Unlike other stationary PV systems, the PV system on the rooftop of a train is movable. Due to this, the angle of solar radiation, global solar irradiance, and temperature on the PV Panel vary as the train moves through its route. To account for this distinctive characteristic and accurately estimate the system's energy output, this research utilizes hourly irradiance data that takes into account the specific time and location of the train's journey. This consideration makes the energy production estimation more realistic than taking a monthly average of the whole route or the whole country.

Therefore, to estimate solar irradiance on the train rooftop first, the location area that the train will spend each hour during operation is obtained from the train operation schedule. Secondly, to calculate the amount of solar radiation on a semi-cylindrical rooftop, the area of the rooftop was divided into smaller areas. The summation of solar energy gain in those areas gives the total radiation on the rooftop of the train. The tilt angle of the PV panels is calculated from the curved structure of the train roof.

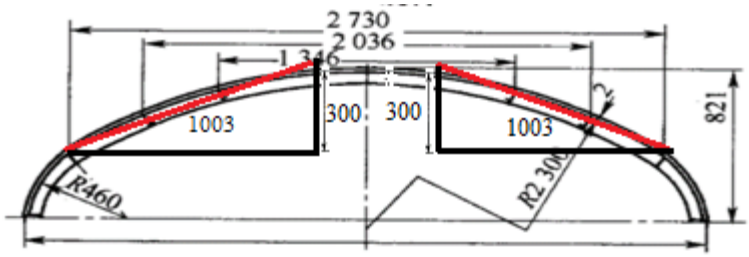

Figure 3. 2 YZ25G Passenger Train Roof Size

The red line indicates the designated location for a PV panel. To determine the tilt angle of the PV, the height (300 cm) is divided by the hypotenuse (1003), resulting in the sine of the right-angle triangle (0.299). Taking the arcsine of this sine value gives the tilt angle of the PV panels, which is calculated to be 17.39 degrees.

Third, azimuth is calculated from the direction the train is traveling. Consecutive departure and arrival points that the train reaches within an hour are inserted into an online bearing calculator [64] to calculate the direction of the train movement.

$$\theta = \operatorname{atan2}(\sin \Delta\lambda \cdot \cos \varphi_2, \cos \varphi_1 \cdot \sin \varphi_2 - \sin \varphi_1 \cdot \cos \varphi_2 \cdot \cos \Delta\lambda) \quad (3.1)$$

where θ azimuth angle, φ is latitude, λ is longitude, φ_1, λ_1 is the start point, φ_2, λ_2 the endpoint, $\Delta\lambda$ is the difference in longitude.

The azimuth angle is utilized to ascertain the orientation of the train roof in relation to cardinal directions. A north-facing position is denoted by 180°, a south-facing position by 0°, a west-facing position by 90°, and an east-facing position by 270°. Finally, hourly irradiance data for locations where the train will spend each hour during operation is obtained from PVGIS [59] for consecutive five years and the average value of those years is considered for the solar energy assessment.

Irradiance on the Rooftop of the Trains for Different Departure Time

To design a rooftop PV system, the abundance of solar energy should be assessed. Therefore, unlike other research done on EDR, irradiance in each area that the train travels within an hour was assessed. Due to different irradiation levels through the route of EDR, different departure time determines the total energy received by the panels. The monthly average daily irradiance variation for different departure times and departure locations is presented below.

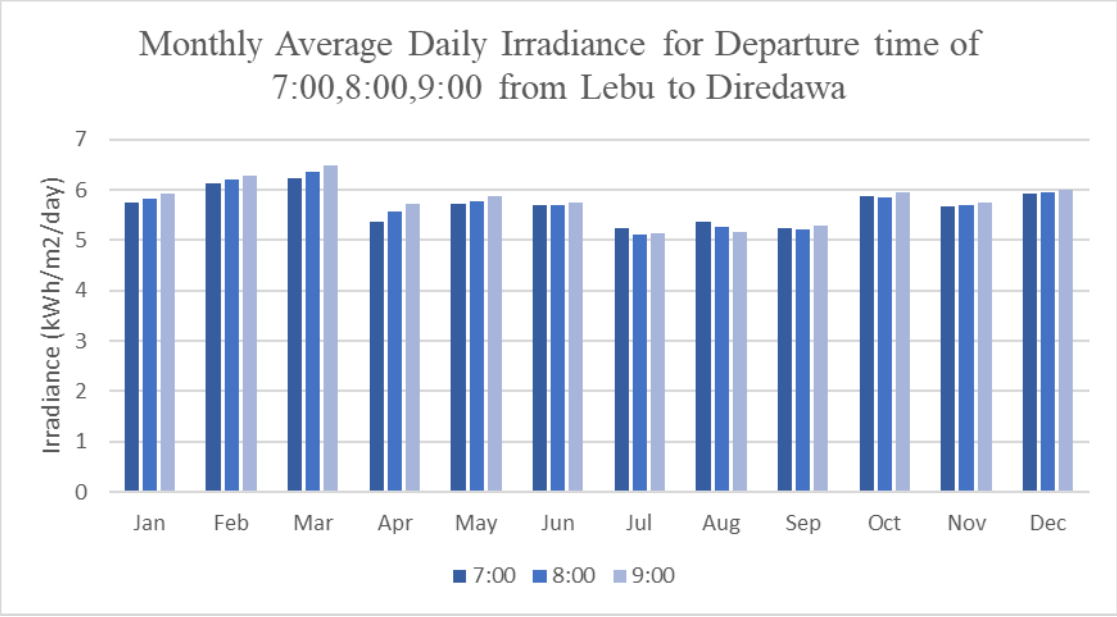

Figure 3.3 Monthly Average Daily Irradiance that can be Received by a Train that Departs at 7:00, 8:00, 9:00 from Lebu to Diredawa

Figure 3.3 shows the monthly average daily irradiance that can be received by a train that departs from Lebu and goes to Diredawa for different departure times. Throughout a year, on average 5.62 kWh/m^2/day, 5.64 kWh/m^2/day & and 5.70 kWh/m^2/day irradiance is received by the panels for departure times of 7:00, 8:00, and 9:00 respectively. The result shows a train that departs at 9:00 from Lebu receives the highest total daily irradiance. This is because a train that departs at 7:00 spends less morning time in areas near the departure location (Lebu, Bishoftu & Adama) and spends most of its afternoon around its departure location (Diredawa) irradiance; on the contrary, a train that departs at 9:00 spends smaller time at the arrival location in the afternoon. The irradiance in the afternoon at Diredawa is smaller when compared to its neighboring areas towards the departure areas (towards the West of Diredawa). However, during the summer months (July and August) the highest total irradiance is received at 7:00; this is mainly because, the months are rainy and cloudy in the areas near the departure location (Addis Ababa, Bishoftu, Adama).

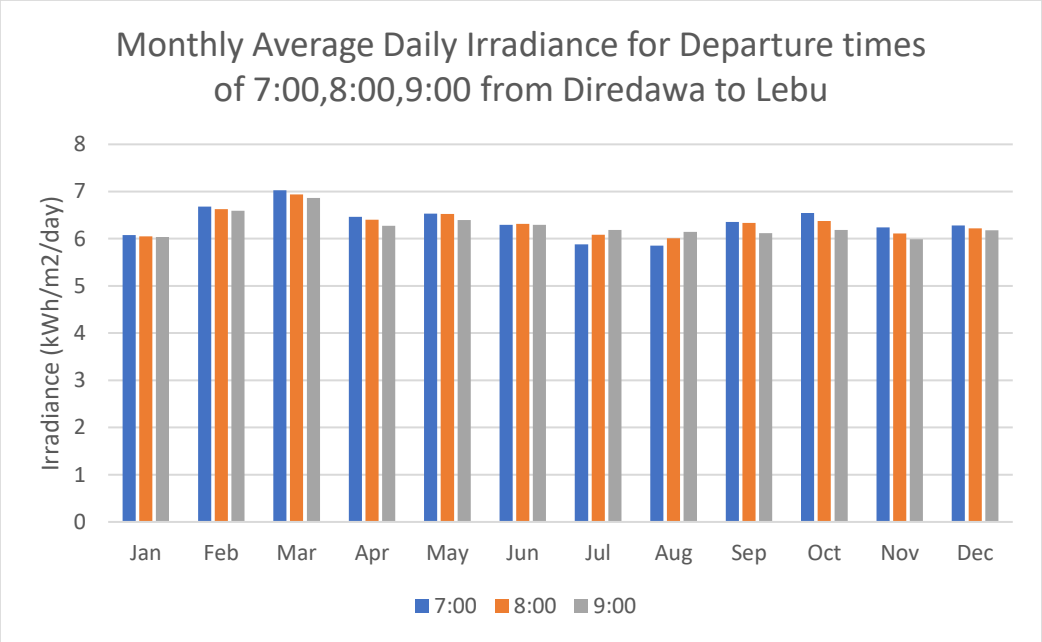

Figure 3.4 Monthly Average Daily Irradiance that can be Received by a Train that Departs at 7:00,8:00,9:00 from Diredawa to Lebu

Figure 3.4 shows the monthly average daily irradiance that can be received by a train that departs from Diredawa and goes to Lebu for different departure times. The result shows the train that

receives the highest amount of irradiance throughout the day is the one that departure at 7:00 relative to other trains that depart at 8:00 & 9:00. This is because the hourly irradiance near the destination is higher in the afternoon, and a train that departs at 7:00 will spend longer time in the afternoon at the destination (Lebu). However, during the summer months (July and August) the highest total daily irradiance is received for a train that departs at 9:00 this is mainly because the months are rainy and cloudy in the arrival area (Addis Ababa, Bishoftu, Adama).

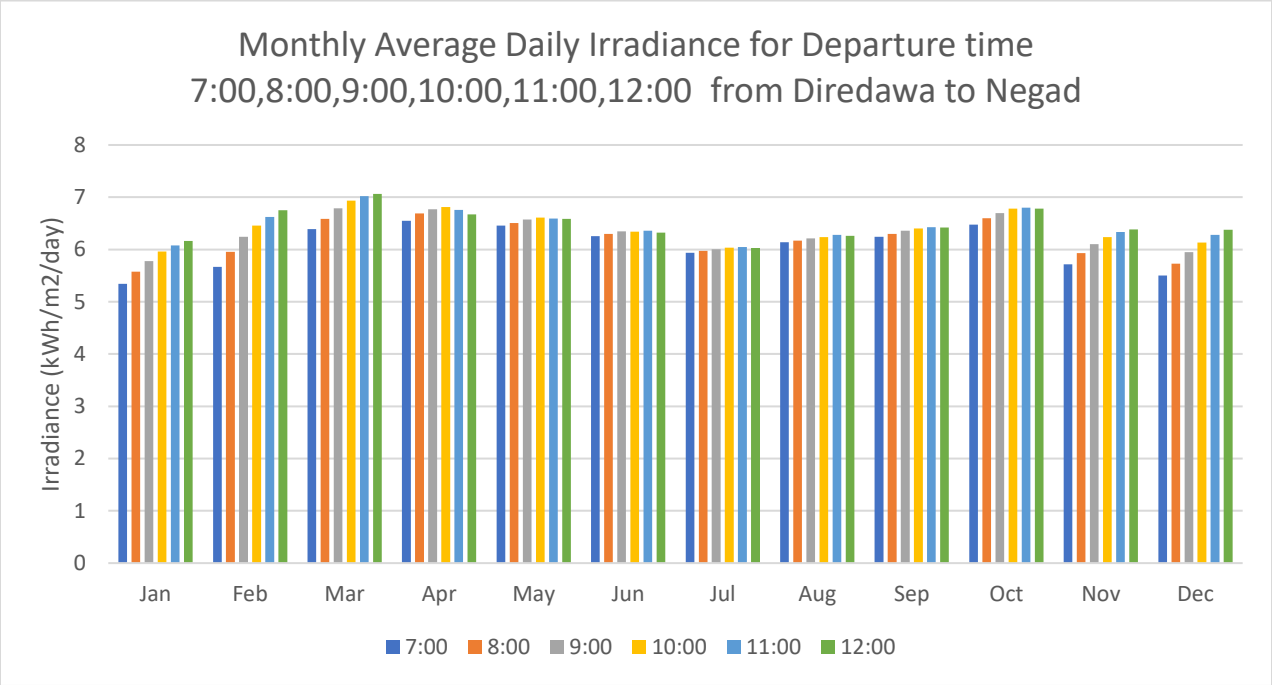

Figure 3.5 Monthly Average Daily Irradiance that can be Received by a Train that Departs at 7:00 -12:00 from Diredawa to Negad

Figure 3.5 shows the monthly average daily irradiance that can be received by a train that departs from Diredawa and goes to Negad for different departure times. The result shows the train that receives the highest amount of irradiance throughout the day is the one that departure at 12:00. This is because the hourly irradiance near the destination is lower in the afternoon, and a train that departs at 12:00 will spend smaller time in the afternoon at the destination (Negad). In other words, a train that departs at 7:00 has a lower sunshine period. This is because a train that departs at 7:00 reaches its destination earlier, however, the sun sets earlier at the destination since the destination is located East of the departure location.

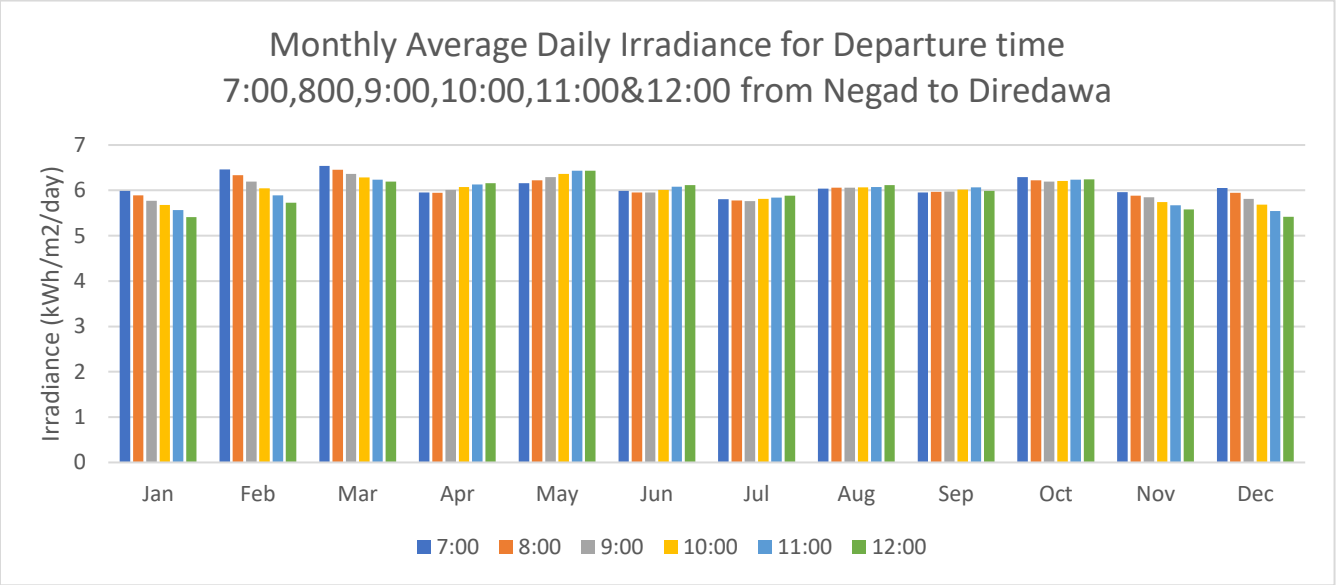

Figure 3.6 Monthly Average Daily Irradiance that can be Received by a Train that Departs at 7:00 -12:00 from Negad to Diredawa

Figure 3.6 shows the monthly average daily irradiance that can be received by a train that departs from Negad and goes to Diredawa for different departure times. The result shows the train that receives the highest amount of irradiance throughout the day is the one that departs at 7:00 from Negad. This is because the hourly irradiance near the destination is higher in the afternoon, and a train that departs at 7:00 will spend a longer time in the afternoon at the destination (Diredawa). In other words, a train that departs at 7:00 has a higher sunshine period this is because it reaches its destination earlier, however, for the rainy months of the destination a train that departs at 12:00 will receive higher daily total irradiance.

Since the travel between Diredawa and Negad takes only five hours, a train that departs from the departure location will arrive at its destination and return to its departure location within a single day. For the travel between Diredawa and Negad, there are two possible departure locations and times; the first one is from Diredawa to Negad at 7:00 and back to Diredawa. The second one is from Negad to Diredawa at 7:00 and back to Negad. Figure 3.7 shows that departing from Negad at 7:00 to Diredawa and returning to Negad at 12:00 enable the PV panel to receive the highest

irradiance since departure times 7:00 from Negad to Diredawa and 12:00 from Diredawa to Negad are the best departure times as shown in Figure 3.5 and Figure 3.6.

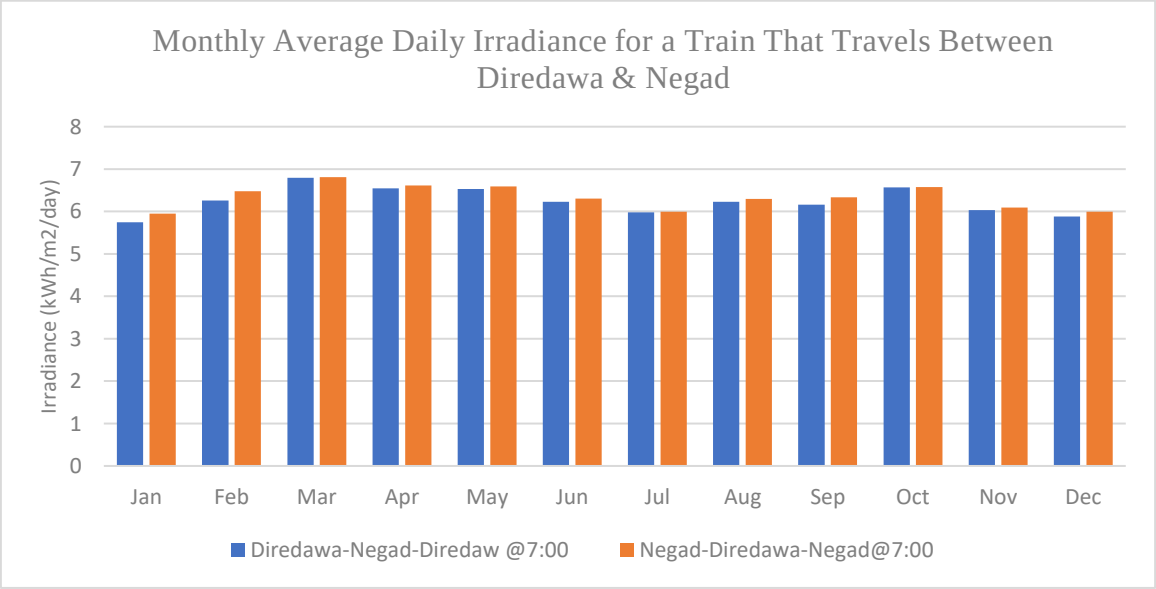

Figure 3.7 Monthly Average Daily Irradiance for a Train that Departs at 7:00, from Diredawa to Negad & back to Diredawa at 12:00

Generally, the data collected shows that areas through the Ethio-Djibouti railway route have a good potential for the PV system with monthly average daily irradiance values ranging from 5.3kWh/m^2/day to 7kWh/m^2/day. The data also shows the departure time of a train determines the total daily irradiance received by the train. The best departure time to receive the highest total irradiance; for a train that departs from Lebu to Diredawa is 9:00, for a train that departs from Diredawa to Lebu is 7:00, for a journey between Diredawa and Negad a train that departs from Negad to Diredawa and back to Negad is 7:00 receives the highest irradiance.

The amount of total irradiance received determines the energy output of the PV system and therefore the power and energy production are analyzed in the next sections.

3.2 Energy Production and Energy Requirement Analysis

In designing a PV system, calculating the energy requirement of the system and the energy generation capacity of photovoltaic panels in a particular location is the basic step to match the demand and supply. However, the PV system for a train rooftop has limited PV panel weight

standing capability and limited installation area. So, to design a PV system for a train rooftop, the following sequential procedure was followed:

First, the area where the panels can be fixed is calculated.

Secondly, PV panels with higher efficiency are chosen to generate more power while utilizing limited space. These panels are also lightweight to avoid additional costs for traction power. Moreover, they have a relatively lower cost, ensuring that their feasibility is not compromised.

Thirdly, the power that can be generated is calculated, and then the total energy captured for a day and a year is calculated.

Finally, depending on the PV generation capacity, the electrical load to be served by the PV system is selected.

3.2.1 Effective Area Calculation and PV Array Sizing

In the case of rooftop PV system design, the surface area of a train car roof is a fixed parameter in the calculation and sizing of the PV array.

The total area of the roof of an Ethio Djibouti passenger train couch is

$$A_T = 25.5\text{m} \times 3.105\text{m} = 79.1775\ \text{m}^2$$

Where A_T is the total area of the roof.

To calculate the effective area in which the PV panels will be installed, the spacing between modules, walkways, space for fixing access, and maintenance access should be taken into account.

$$A_{eff} = A_T - A_w - A_{AC} \quad (3.2)$$

$$A_{AC} = 3\text{m} \times 3.105\text{m} = 9.315\text{m}^2$$

$$A_w = 0.9\text{m} \times 22.5\text{m} = 20.25\text{m}^2$$

Where A_{eff} is an effective area for fixing PV panels, A_w is an area for walkway and fixing access and A_{AC} is an area covered by an Air conditioner at the roof

If the values of A_T, A_w, and A_{AC} are substituted in Eq. 3.2, the effective area for fixing the PV panel on a single couch becomes 49.65m^2. And EDR has a plan to have 60 passenger couches at the end of 2016 EC [65]. Therefore, the total available area to install PV panels will be 2979 m^2.

After knowing the area available for PV panel installation, finding a high-efficiency PV panel that generates higher power within the available area is the next thing to do.

Different solar panels with up to 25% efficiency which have been developed recently are already available in the market [66]. Among the available PV modules, DSM370(Q) from Wuhan Rixin Technology Co., Ltd PV module [67] is selected because of its smaller size to fit on the available area and lighter weight to reduce traction load. Additionally, the flexible structure to install on the rooftop easily and higher efficiency to generate maximum power within the area available make it more advantageous. The specification of the module is shown below in Table 3.1.

Table 3. 1 Datasheet for the 370W Monocrystalline Module of DSM370(Q)

Electrical Specifications (STC)	Maximum Power	Maximum power Voltage	Maximum power Current	Open Circuit Voltage	Short Circuit Current	Efficiency
DSM370(Q)	370W	33.6 V	11.01 A	40.2 V	12.13 A	21%

Mechanical Specifications	Power Temperature Coefficient	Voltage Temperature Coefficient	Current Temperature Coefficient	Length, Width	Weight per panel
DSM370(Q)	-0.38%/ c^o	-0.28%/c^o	0.02/c^o	1.74m x 1.03m	5.8kg

The area of one panel is then given by:

$$A_P = 1.740\text{m} \times 1.030m = 1.7922\text{m}^2.$$

Where A_P is the panel area.

The train's roof is 3.105m wide, which allows for two panels to be placed side by side. The length of the train is 25.5m, which can accommodate twelve panels placed end to end. So, the

available area on the train's roof can hold up to twenty-four, DSM370(Q) PV modules. Therefore, when considering all 60 passenger couches, the total number of panels that can fit on the roofs of these couches is 1440.

3.2.2 Effect of Shading Temperature and Additional Weight on Energy Consumption

In the case of EDR, most of the paths taken by the trains are located in rural and desert areas. Therefore, there are no big construction, dens that shade the PV panels. Even if there are some hills and some trees through the path, the train could be shaded for minutes which is a very small time to consider as a shading when compared to a ten-hour journey.

According to a US solar supplier [68], heat can reduce the output power of solar panels by 10%-25%, depending on the location temperature. Solar panels produce the best output power at an optimal temperature of 25 degrees Celsius (77 degrees F). As the temperature increases, the open circuit voltage decreases at a larger rate while the short current output increases slightly.

Fortunately, in the case of a train rooftop PV system, the PV panel will be naturally ventilated by the wind due to the relative motion of the wind and the trains. The PV panel on the rooftop of a train is ventilated by the wind. Additionally, the cooling system of the train sucks hot air and releases cold air through a duct which is right under the roof of the train. Therefore, the cooling system of the passenger trains will also contribute to the colling of the PV panels. Furthermore, the installed solar panel will reduce the temperature of the train, as the panel converts some of the irradiance to electric power, which would otherwise increase the temperature of the train. This implies that the panel’s temperature is mostly maintained near room temperature [69] and that it will also reduce the train’s energy consumption for air conditioning of the passenger couches.

It is important to assess the structural capacity of the roof before installing PV panels to ensure its safety. This involves considering the weight of the panels per unit area in relation to the maximum load that the roof can bear, which is 97.6 kg/m^2 [12]. To reduce the risk of structural failure from unforeseen factors like water or wind, it is advisable to have a safety factor of 4 for rooftop PV systems [12]. Therefore, the maximum allowable load on the rooftop becomes 24.4 kg/m^2. The additional weight of the PV panels on the roof is 3.24 kg/m^2 if all 24 panels are

installed on the rooftop of the train. Therefore, installing the PV panels on the roof does not pose a risk of overloading because the extra weight from the panels is very low compared to the standard limit.

Even if, the rooftop of the trains can withstand the weight of the panels easily, installing solar panels on the roof of the train increases the total weight of the train. This in turn increases the energy consumption (EC) of a train for traction purposes. Hence, the energy consumed due to the additional weight of the panels must be calculated.

However, to be efficient, a solar system must generate significantly more energy than the extra energy used due to the added weight. To lower energy consumption from the weight of a PV system, a PV panel weighing 5.8kg was chosen as it is 70% lighter than a traditional glass module.

The total additional weight on a passenger train includes the weight of the PV panels, the weight of a supporting structure, and the weight of the designed DC-DC convertor which are 104.4kg (Considering 18 DSM370(Q) PV panels), 5 kg, and 4 kg respectively. Therefore, the total added weight due to the PV system is 113.4 kg.

The additional energy consumed due to the PV panels can be calculated by multiplying the specific energy consumption with the added weight on a train and the distance traveled.

Specific energy consumption is the energy consumed from a power supply per ton mass of a train per km length of the run.

$$\text{Specific energy consumption} = \frac{\text{Specific energy output}}{\eta} \tag{3.3}$$

Where η is the overall efficiency of the transmission gear and motor.

$$\text{Additional energy consumption} = \text{Specific energy consumption} \times \text{addtional weight} \times \text{distance traveled} \tag{3.4}$$

The measured value of specific energy consumption for EDR passenger trains ranges from 200 to 300 kilowatt-hours per 10,000ton-km.

Therefore, using Eq. 3.3, the resulting increment in energy consumption is 1.57 kWh per couch for the 462km travel between Lebu and Diredawa and 0.99kWh per couch for 291km travel

between Diredawa and Negad. This amount of energy is very small compared to the daily energy production of the PV system. The energy consumption due to this additional weight is not only small but also some amount of the energy lost can be compensated by the panels' contribution to reducing air conditioner power consumption. Additional weight due to the PV panels also adds energy that can be produced by regenerative braking.

Therefore, the additional energy consumption of a train due to the additional weight of the PV system is very low. However, this additional energy consumption is subtracted from the energy production of the PV system to get the net and precise output energy of the PV system. However, the effect of temperature and shading are neglected because their effect is very small and do not worth further calculation and analysis.

3.2.3 Energy Production Estimation

After knowing the abundance of solar energy in the area, calculating the effective available area for PV panel installation, and selecting an efficient PV module, the next thing done is estimating the energy production capacity.

This research collects hourly irradiance data for every location where the trains hourly arrive. So, energy production is calculated by considering in which area the train is and at what time this train has arrived at that location. The location and time of departure of the trains are obtained from an operational schedule of Ethio-Djibouti railways.

After hourly irradiance data for the whole route had been collected, the next step was calculating the output power and daily energy production of the selected PV panel. The PV output power was calculated using Eq. (3.4) as used in HOMER pro software which is widely used software in PV system design [70].

$$P_{pv} = Y_{pv} \times f_{pv} \times \left(\frac{G_T}{G_{T,STC}}\right)\left[1 + \alpha_p\left(T_C - T_{C,STC}\right)\right] \tag{3.5}$$

Where, f_{pv} is the PV derating factor [%], which is usually between 0.5 and 0.9 and accounts for such factors as soiling of the panels, wiring losses, aging, shading, snow cover, and so on.

Y_{pv} is rated power output of a PV panel under standard test conditions (STC) [kW].

G_T is the solar radiation incident on the PV array in the current time step [kW/m^2].

$G_{T,STC}$ is the incident radiation at STC [1 kW/m^2].

α_p is the temperature coefficient of power [%/°C].

T_C is the PV cell temperature in the current time step [°C].

$T_{C,STC}$ is the PV cell temperature under STC [25 °C].

For the case of Ethio-Djibouti railway passenger trains the PV panels are well ventilated due to the wind and air condition system of the passenger train. Due to these conditions, PV cell temperature is equal to PV cell temperature under STC. Therefore, Eq. 3.5 can be further simplified [70] to Eq. 3.6.

$$P_{pv} = Y_{pv} \times f_{pv} \times \left(\frac{G_T}{G_{T,STC}}\right) \tag{3.6}$$

The daily energy production of the PV system can be calculated as shown in Eq. 3.6.

$$E_{pv} = P_{pv} \times t \times n \tag{3.7}$$

Where, E_{pv} is PV energy production, P_{pv} is the PV power; t is the unit time that the train operates; n is the number of panels.

Maximum output power during maximum irradiance from a single PV panel is equal to

$$P_{pv} = 370\ W \times 0.85 \times \left(\frac{1060\ W/m^2}{1000 W/m^2}\right) = 333W$$

If all the effective area of a couch rooftop is covered with 24 panels, the maximum power that can be generated will be 7992W. And the maximum power for the total 60 couches will be 479.52kW.

The energy production of the rooftop PV system varies with the departure time of the train, so energy production of different departure times was evaluated to show that departure time has a crucial role in determining the amount of energy production of the photovoltaic panels. The departure times 7:00, 8:00 & 9:00 were selected for comparison on the trains that travel between

Diredawa and Lebu, and departure times 7:00 from Diredawa - Negad – Diredawa and Negad – Diredawa - Negad were evaluated for the case of an international journey between Diredawa and Negad.

Section 3.1.2 showed that the departure time of the train determines the total daily irradiance received by the PV panels. The energy production of the PV system is determined by the amount of irradiance received by the panels. This implies the daily energy production of passenger couch rooftop PV systems will also vary with departure times and departure locations.

Therefore, this section presents the calculated monthly average energy production of a single-passenger train rooftop PV system for different departure times and locations. The energy production represents the expected energy output in the middle of the solar panels' lifetime (during the 12th year) since the efficiency of the solar panels reduces their efficiency by 0.6% every year due to aging.

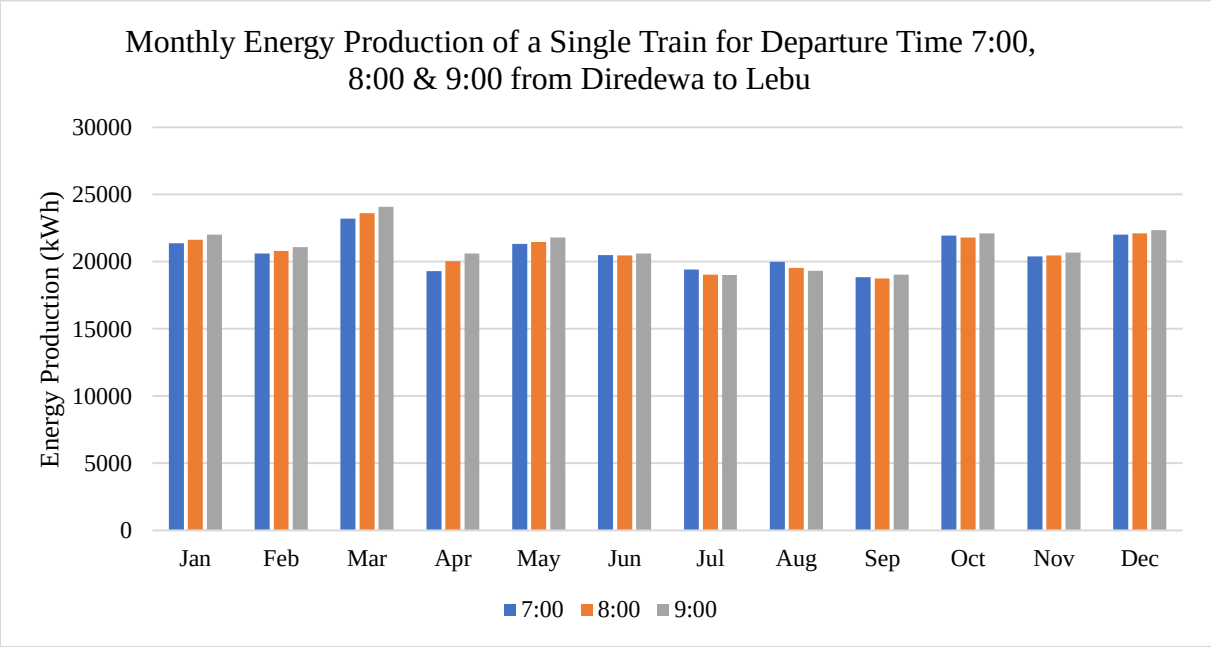

Figure 3. 8 Monthly Energy Production of a Single Train for Departure Time 7:00, 8:00, and 9:00 from Lebu to Diredawa

Figure 3.8 shows the monthly energy production of a single train that departs from Lebu to Diredawa at different departure times. As expected, the result shows a train that receives the highest amount of irradiance throughout the month produces the highest energy production.

Total yearly energy production for a train that departs from Lebu at 7:00, 8:00, and 9:00 and goes to Diredawa is 248.866 MWh, 249.640 MWh & 252.698 MWh respectively. As shown in Figure 3.8 the difference in energy production for the three-departure time is small for the Lebu Diredawa case. However, if this small difference is considered for the lifetime of the PV system; the difference becomes a considerable amount of energy, therefore a train that departs from Lebu station and travels to Diredawa at 9:00 collects higher energy.

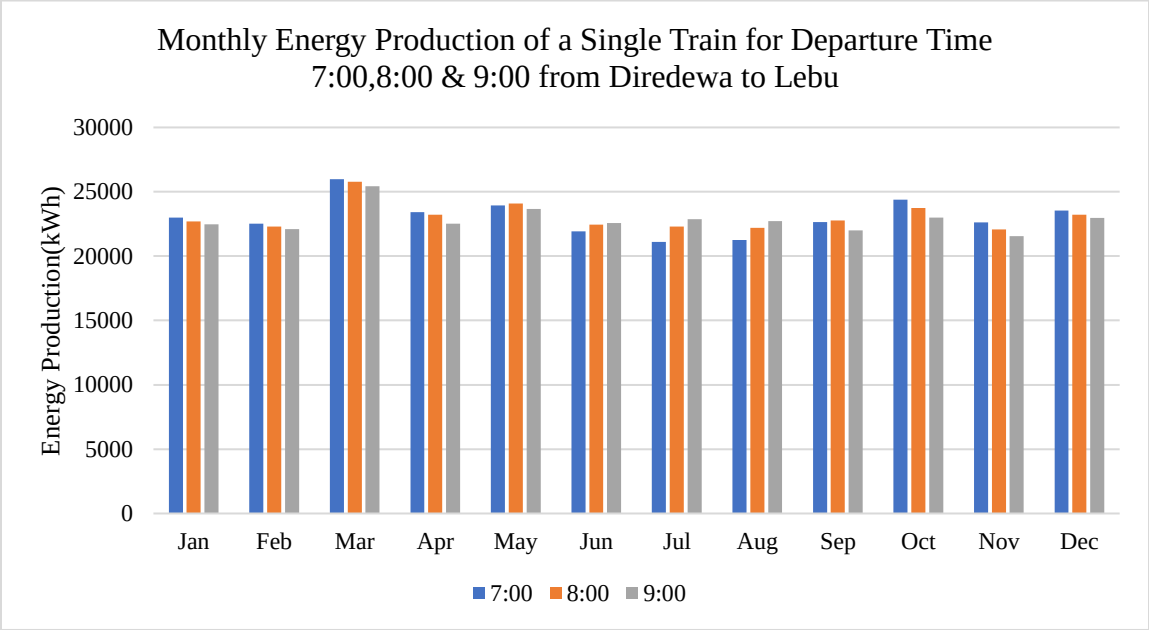

Figure 3. 9 Monthly Energy Production of a Single Train for Departure Time 7:00, 8:00, 9:00 from Diredawa to Lebu

The total yearly energy production of a train that departs from Diredawa at 7:00,8:00 & 9:00 and goes to Lebu is 277.836MWh, 277.085MWh, and 273.818MWh respectively. As shown in Figure 3.9 the difference in energy production for the three-departure time is small for the Lebu Diredawa case. However, if this small difference is considered for the lifetime of the PV system the difference becomes a considerable amount of energy, therefore the best departure time for trains that depart from Diredawa station and travel to Lebu is 7:00.

Section 3.1.2 shows that a train that departs from Negad at 7:00 and a train that departs from Diredawa at 12:00 receives the highest monthly irradiance. This implies maximum energy can be harvested, from a train that travels from Negad to Diredawa and back to Negad, when the train

departs from Negad at 7:00 and then returns from Diredawa after 12:00. Therefore, energy that can be harvested for the whole trip is calculated and shown on the Figure 3.10, for the previously stated departure times only.

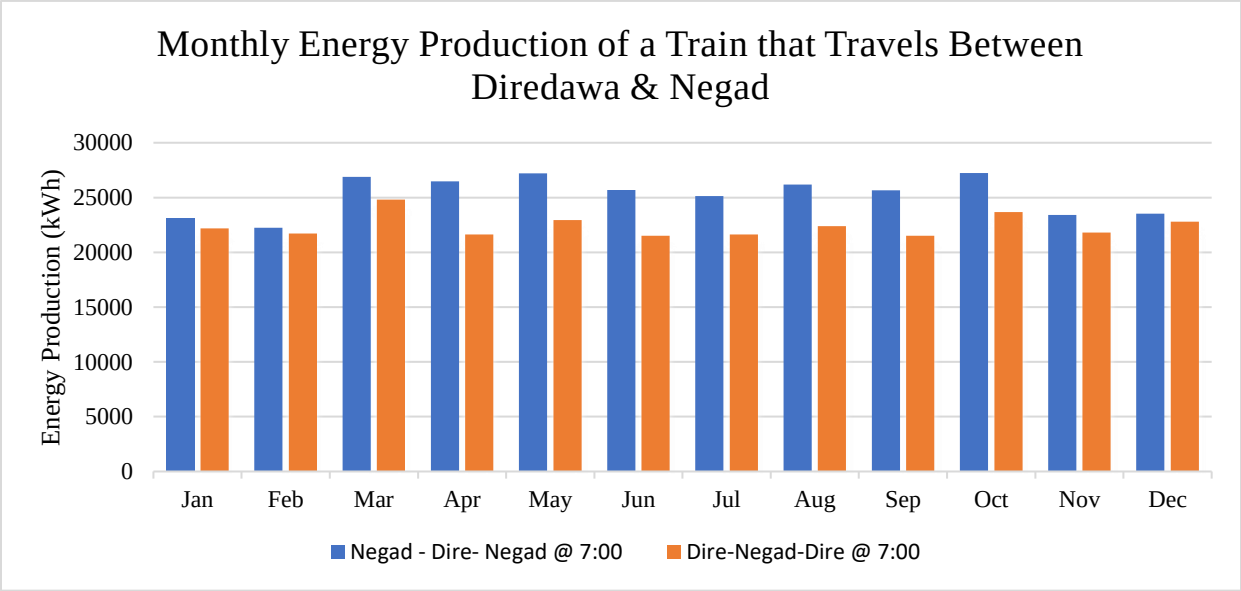

Figure 3.10 *Monthly Energy Production of a Train that Travels Between Diredawa & Negad*

Figure 3.10 shows the monthly energy production of a train that travels between Diredawa & Negad for different departure locations & times. The total yearly energy production of a train that departs from Diredawa at 7:00 to Negad and back to Diredawa is 268.63 MWh per year; whereas a train that departs from Negad at 7:00 to Diredawa and back to Negad 302.81MWh per year, Therefore, the highest energy is collected by a train that depart from Negad at 7:00 to Diredawa and to return to Negad at 12:00.

According to the available irradiance, the average daily energy productions of a single passenger coach rooftop PV system from different departures at different departure locations are shown in Table 3.2 below

Table 3. 2 Average Daily Energy Production of a Single Passenger for Different Departure Locations and Departure Times.

Departure time / Locations	7:00	8:00	9:00
Lebu to Diredawa	34.09kWh/day	34.12kWh/day	34.62kWh/day
Diredawa to Lebu	38.06kWh/day	37.96Wh/day	37.51kWh/day
Diredawa -Negad -Diredawa	36.80kWh/day		
Negad - Diredawa -Negad	41.48kWh/day		

3.2.4 Energy Requirement of the System

The total power requirement of a train at specific time is represented by Eq. 3.8, where the power used by the i_{th} couch at time 't' is denoted by P_i, and 'n' signifies the count of couches in operation. The total energy (E_t) needed for the duration from t1 to t2 is expressed by Eq.3.9.

$$P_t = \sum_{i=1}^{n} P_i \tag{3.8}$$

$$E_t = \sum_{i=1}^{n} \int_{t1}^{t2} P_i \, dt \tag{3.9}$$

Each passenger train couches of EDR gets a power supply from a locomotive through a 600V DC busbar. This 600V DC power is connected with invertors, to supply AC loads, and a DC-DC converter to supply DC loads of the couches. Each AC and DC load of a passenger couch is stated in Appendix II, along with their voltage and power rating.

The AC loads are supplied from a 35kVA invertor whereas the DC loads are supplied from a DC-DC convertor and charger controller with a capacity of 8kW. When the power supply is normal, power from 35kVA inverters offer power to the air conditioning units, electric water heaters, and other AC loads. The DC charger controller takes DC 600V from the bus bar and converts it to 110V DC to charge the two batteries with 120AH capacity and supply DC auxiliary loads. The output of the charger controller is connected to the DC110V bus bar to supply DC loads like the lighting, power controller, axle temperature sensors, and the anti-skid device are connected.

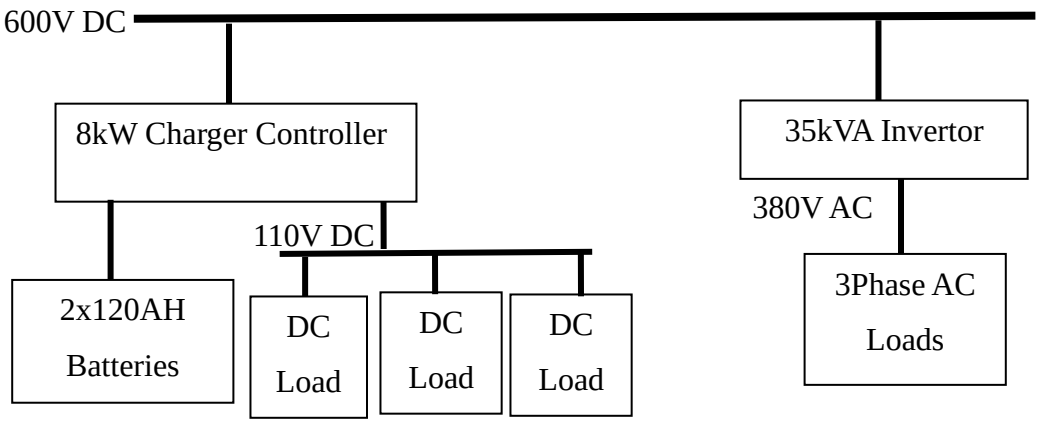

Figure 3. 11 Block Diagram of EDR Passenger Train Couches Power System

3.3 PV System Design

Because of the limited PV installation area and efficiency of PV panels, the energy generated by the train rooftop PV system can supply only devices that are supplied from an 8kW charger controller. These devices have a very essential role in train operation, passenger comfort, and passenger safety.

The 8-kW charger converter supplies the batteries with charging current up to 30A and loads connected to 110V DC bus bar up to 4.5kW loads. From these loads, 1.5 kW supplies the lighting load which is used only at night time. The remaining 3kW power is used by devices that need an uninterrupted power source as long as the train is operating. The 110V DC power supply is mainly used to provide power for anti-skid devices, power conversion control, air conditioning unit control, under voltage protection of storage battery, lighting controller, signaling devices, and the centralized axle temperature-alarming device. The DC power supply also provides power to the programmable logic controller (PLC) which receives all kinds of orders through a microprogrammable terminal and takes the corresponding operation steps automatically. The PLC also detects, indicates, and protects all kinds of faults caused in the process of operating the electrical system promptly.

According to the operational schedule of the EDR passenger train, it takes 10 hours to travel from Lebu to Diredawa or from Diredawa to Lebu. Therefore, if the train only operates during

the day, each couch requires 30 kWh of energy per day. However, if we consider that the train operates for two hours during the night and uses lighting, an additional 3 kWh of energy is needed for each couch. This results in a total energy requirement of 33 kWh per day for a single couch. Considering that 40 passenger couches are operating between Lebu and Diredawa, the total energy requirement per day for this route is 1.32 MWh.

In the case of international travel, it takes 5 hours to travel from Diredawa to Negad, and it takes another 5 hours to return to Diredawa. The same is true for a train departs from Negad to Diredawa and back to Negad. In addition to this, an extra one hour is spent on the border between the two countries and when returning to departure location. Therefore, totally the train operates for 11 hours. This implies that 33 kWh per day of energy is required for a single couch if the train operates only throughout the day. However, if we consider the train operates for two hours of the operation time during dark times and the passenger uses light the total energy requirement for a single couch will be 36 kWh per day. Since 20 passenger couches operate between Diredawa and Negad the total energy required becomes 0.72MWh per day.

3.3.1 PV Panel Sizing

After estimating the generation capacity of the train rooftop PV system and determining the load to be served by the PV system, the subsequent task involves selecting the appropriate size of PV panels and establishing the electrical connection between the PV system and the electrical component of the passenger coaches.

According to the findings in section 3.2.4 of this research, the loads that can be served by the PV system are 110 V DC loads. These 110V DC loads are powered by a DC-DC converter (charge controller) in each passenger couch. To power these components by the PV system the output power and voltage of the PV system must be regulated. To regulate the voltage and to control power flow efficiently DC-DC convertor with an MPPT is designed.

The findings in section 3.2.4 of this research also state that each couch requires a power output of 4.5kW and an energy consumption of up to 36 kWh per day. To ensure that the loads receive adequate energy based on the amount of solar radiation available, 18 PV panels are necessary for a single couch. To make the voltage rating of the charger controller and the output of the PV

array compatible, minimize power loss, and obtain sufficient power, the 18 PV panels on each couch are connected in series. This arrangement results in a maximum power output voltage of 604.8 V, a maximum power current of 11.01A, and a maximum power output of 6660W at standard test conditions. However, unlike power from the pantograph, the power and voltage output of a PV panel vary based on the amount of sunlight it receives. It is crucial to ensure that this variation does not pass the threshold voltage and current value of the passenger couch electrical component nominal voltage and current valve which are plus and minus five percent (as stated in the operation manual of the EDR passenger coaches). So, it is necessary to design an appropriate control system for the PV system based on the input voltage and the required output power.

The PV systems controller must not only control the output power and voltage of the DC-DC converter but it must also control the discharging and charging process of the two 120AH batteries. This allows for effective management of the energy output from the PV system. During peak sunshine hours, the PV system supplies power to the DC loads, and any extra power generated is used to charge the batteries. However, during off-peak periods when the power generated by the PV system may not be enough, the previously charged batteries are utilized to supply power to the DC loads. If both the PV system and the batteries are unable to meet the load demands of the train, the power system from the overhead contact wire takes over and supplies the necessary power while simultaneously charging the battery. A block diagram representing the integrated PV system with the passenger couch power system is shown in Figure 3.12.

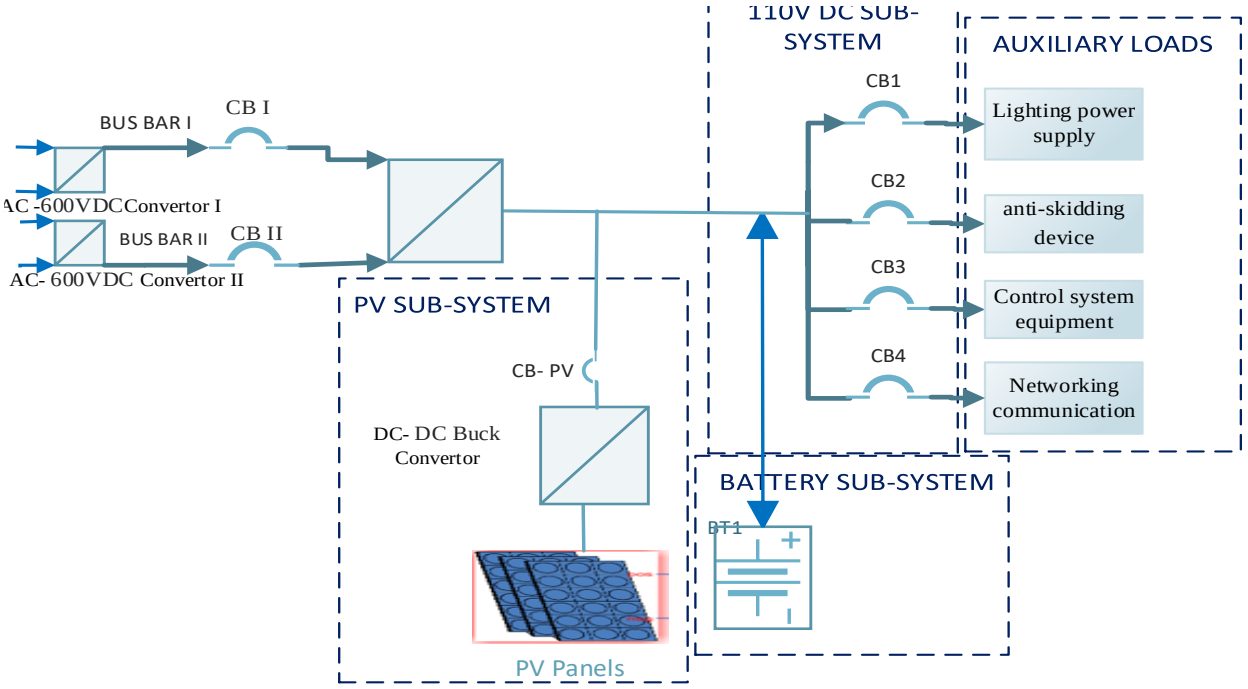

Figure 3. 12 Block Diagram of the Designed Train Roof Top PV System with Battery Backup.

3.3.2 Battery Sizing

A PV system can only supply loads only when there is sufficient irradiance. Therefore, if there is no sufficient irradiance the load must be served through other ways. Fortunately, the passenger couches have two 120AH NiCd batteries with a maximum charge current of 30A, which are installed for emergency power suppling purposes. So, these batteries are not used unless there is total power loss from overhead contact wire. Hence, instead of installing another battery set, these batteries are used for their intended purpose and also as backup energy storage for the PV system. They will be charged when extra power is generated by the PV system and discharged during dark times when there is no sufficient irradiance on the PV panels to supply the DC auxiliary loads. It's important to note that the voltage of the train battery is 110VDC.

When fully charged, the battery autonomy can also be computed using the formula in Eq. 3.10 as indicated [71].

$$number\ of\ autonomy\ hours = \frac{n \times C_b \times k \times V_b}{E_b} \tag{3.10}$$

Where E_b is hourly energy consumption; V_b is Battery Voltage; C_b is battery capacity in Ah; k is the permissible depth of discharge, and n is the number of battery sets.

Even if the installed Ni-Cd battery can discharge totally, 50% of its discharging capacity is used by the rooftop PV system. By using Eq. 3.10 the battery running time has been calculated as 3 hours when it is fully relied on to supply the maximum power of 4.5kW. This implies the batteries can sufficiently supply the three hours of train operation during the dark hours when the PV system cannot produce sufficient power.

3.4 PV System Modeling

To validate the designed system's capability to supply the DC loads of the passenger train couches, the rooftop PV system is modeled and simulated. The model includes PV panels that are connected in series to form an array with an output of desired voltage and power. It also includes a buck converter connected to the array, which supplies the DC loads with the appropriate voltage level. Additionally, there is a bi-directional DC-DC converter with a battery management system that controls the charging and discharging of the batteries based on the battery state of charge and the available power from the PV system. Furthermore, the model also contains a control system that enables the buck converter and DC-DC bidirectional converter to operate in different modes for various scenarios. A detailed explanation of the system and its subsystems' modeling and simulation is provided in the following sections of 3.4.

3.4.1 PV Subsystem

In passenger train couches of EDR, the 600VDC from the main convertor needs be to converted to 110VDC to supply DC loads. This is done using a DC-DC buck converter, the voltage output is controlled by applying the appropriate duty cycle. In the case of the PV system, the buck converter's input is connected to a PV array through an input capacitor which stabilizes PV panel voltage fluctuations. Other than the input capacitor the buck convertor contains IGBT and freewheeling diode for switching purposes, an inductor to supply smooth and continuous current, and an output capacitor to reduce output voltage ripple. The buck converter's input capacitance

C_{in}, output capacitance $C_{o,}$ and inductance L of the convertor are given by the expressions in Eq. 3.10 and Eq. 3.11 respectively [72].

$$L = V_o(V_i - V_o)/f_{sw} \times \Delta I \times V_i \tag{3.11}$$

$$C = \Delta I f_{sw} \times \Delta V \times 8 \tag{3.12}$$

Where V_i is the input voltage; V_o is the output voltage; f_{sw} is the switching frequency; ΔI is the current ripple of the input current; ΔV is the voltage ripple of the output voltage.

A more practical approach is to size the critical inductance by using percentage of peak-to-peak inductor current ripple based on the maximum load current. It is typically 30- 40 percent of output maximum current.

The voltage rating of the switching device is calculated by adding maximum input voltage and maximum forward voltage drop across the diode.

A purely resistive load is used to represent DC loads

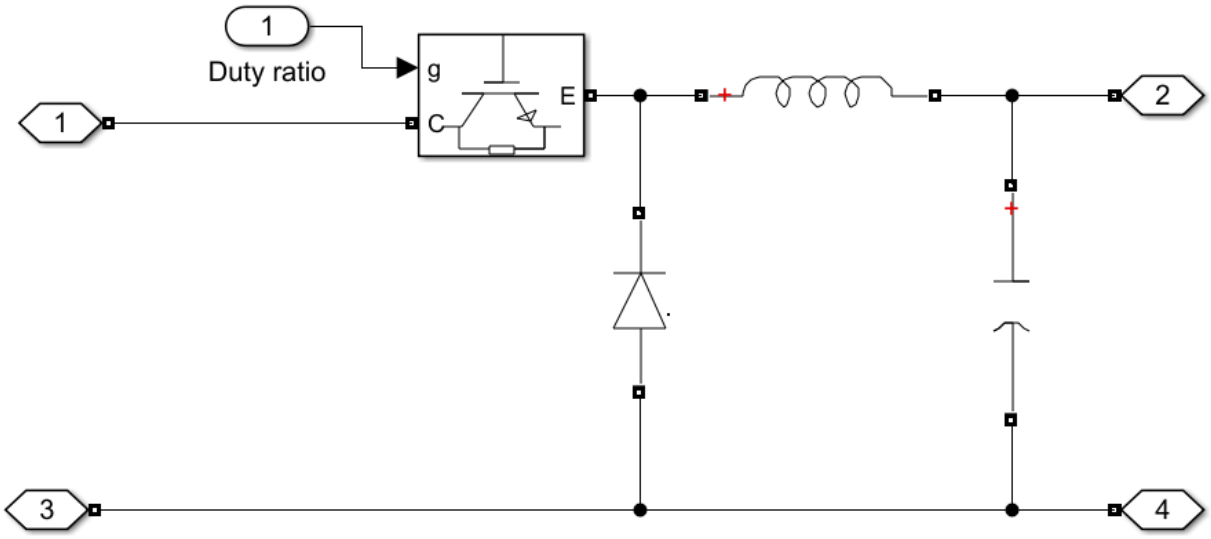

Figure 3.13 Simulink Model of Buck Converter

The PV system's output voltage and power are controlled in two different ways.. The first one is using MPPT which enables the power system to extract maximum power from the PV panels. This mode is selected when the battery is not fully charged and when the irradiance is sufficient

to provide power with at least the minimum output voltage level (96VDC) for the loads. The second mode is the constant voltage control mode. This mode contains an inner current control loop and outer voltage control loop which enables the PV system to provide the DC loads with constant 110VDC and required current. This mode is selected when the battery is fully charged and the irradiance on the PV panels is more than sufficient to provide the DC loads.

3.4.2 The Maximum Power Point Tracking Mode

Although identifying the true maximum power point under changing weather conditions is challenging, various MPPT methods have been created to efficiently locate the MPP. These techniques aim to enhance the solar system's output power even when solar irradiance fluctuates. As indicated in section 2.6, there are different algorithms with different speeds of effectiveness, convergence, sensor requirement, complexity, and installation cost. Among the available MPPT algorithms, the incremental conductance MPPT algorithm indicated in research [58] is selected since it simulated and compared the potential of the PV system using actual situations in Ethiopia and finally showed that the incremental conductance MPPT method is superior for the case of Ethiopia.

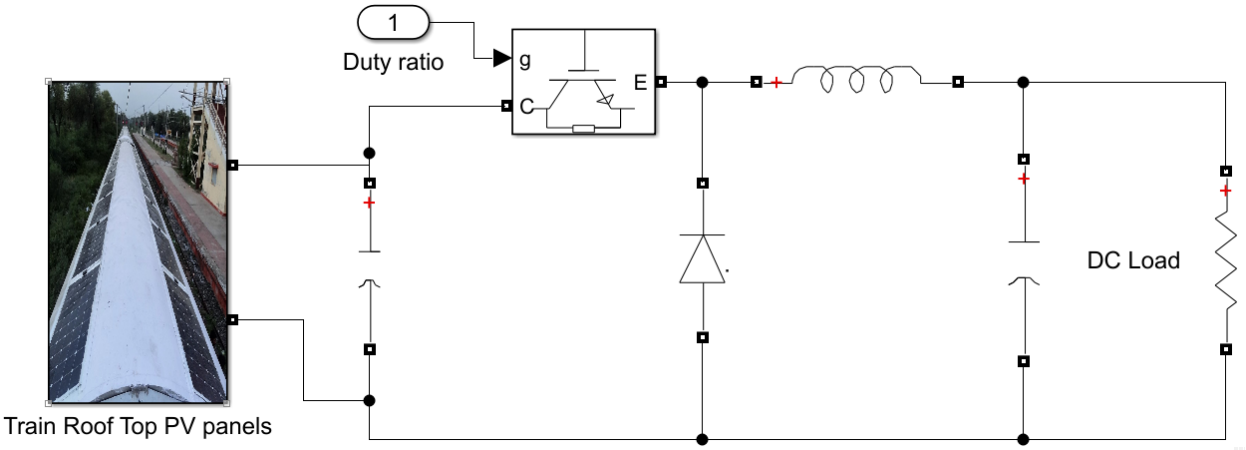

Figure 3.14 Simulink Model of PV Subsystem

3.4.3 Constant Voltage Control Mode

When the battery is fully charged and the photovoltaic (PV) system generates more power than what is required, the output voltage of the buck converter will exceed the nominal voltage range. In such a scenario, it is not recommended for the PV system to operate at maximum power point (MPP). Instead, it should operate in a mode that restricts the PV output power and ensures that the voltage remains within the nominal operating voltage range. To do this, the PV subsystem's output is regulated by a constant voltage controller instead of MPPT. During such situations, the system uses a multi-stage control architecture so that the inner current control and outer voltage control, control the output voltage of the PV subsystem to be 110VDC and the current to be as required by the DC load. The output of the outer voltage loop's determines the current reference signal to the inner current loop, which then generates the duty cycle signal to the PWM generator.

3.4.4 Bidirectional DC-DC Converter

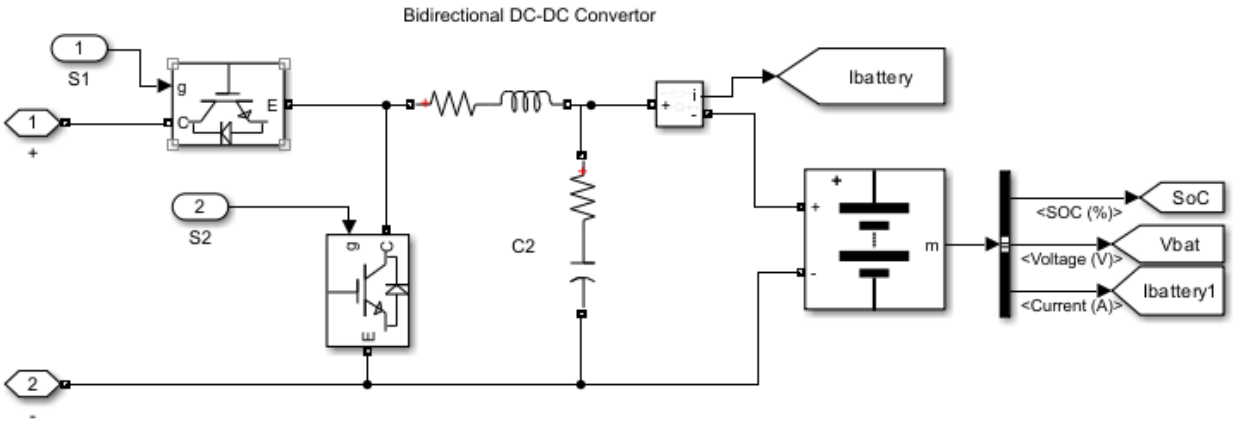

Figure 3. 15 Bidirectional DC-DC Converter Simulink Model

If we assume all components are perfect, both the semiconductor switch and the anti-parallel diode can function as ideal switches. when operated in tandem. When two complementary switches S1 and S2 are alternately turned on and off, a Vpwm switched waveform appears across nodes 1 and 2. The average output voltage Vo is equal to Vpwm and the duty cycle D of the upper switch S1 multiplied by the input voltage Vs.

$$V_o = V_{pwm} = DVs \quad (3.13)$$

To smooth out the output ripple caused by the switched waveform, a filter with components like capacitors and inductors can be integrated. In this context, an inductor is employed to reduce the ripple, allowing the connection to a battery Vb. The nonideal internal resistance R of the inductor is taken into account. At equilibrium, the average current in the inductor is calculated as

$$I_L = \frac{V_o - V_b}{R} \tag{3.14}$$

In situations where Vo is greater than Vb, the inductor current flows from the source Vs to the battery Vb, creating a buck circuit where power is transferred from source to battery.

$$V_o = DV_s \tag{3.15}$$

When Vo equals Vb, the inductor current reaches zero at a stable state, indicating no power exchange between the source and battery. Conversely, if Vo is less than Vb, the inductor current moves from the battery Vb towards the source Vs, establishing a boost circuit where power flows from the battery to the source. Additionally, the relationship between the output voltage Vo and the duty cycles D and D2 of the top and bottom switches follows the equation (3.15).

$$V_L = \frac{1}{1-D_2} V_o = \frac{1}{D} V_o \tag{3.15}$$

D + D2=1 due to the complementary switching of the upper and lower switches.

3.4.5 Battery Management System

The battery management system utilizes a bi-directional DC-DC converter where the battery is charged through a buck converter setup and discharged through a boost converter setup. To enhance battery performance and longevity, systems with battery backup restrict the maximum charging and discharging current. This model constrains the power supplied by the battery to the load and absorbed from the solar PV source using a controller with two loops: an outer voltage loop and an inner current loop.

The output of the outer voltage loop is capped by the maximum charging/discharging current/power limit, introducing non-linearity to the control process. A higher proportional gain in the outer loop voltage controller can cause saturation of the voltage controller even for small

voltage errors, resulting in the controller using on-off control rather than PI control. This situation leads to increased ripple/oscillation in battery charging and discharging current. Conversely, a very low value of voltage PI controller proportional gain may result in a slow response time or failure of the controller to track the reference voltage. Therefore, the proportional gain of the voltage controller and the zero of the PI controller are selected to achieve improved response and lower oscillation in battery current.

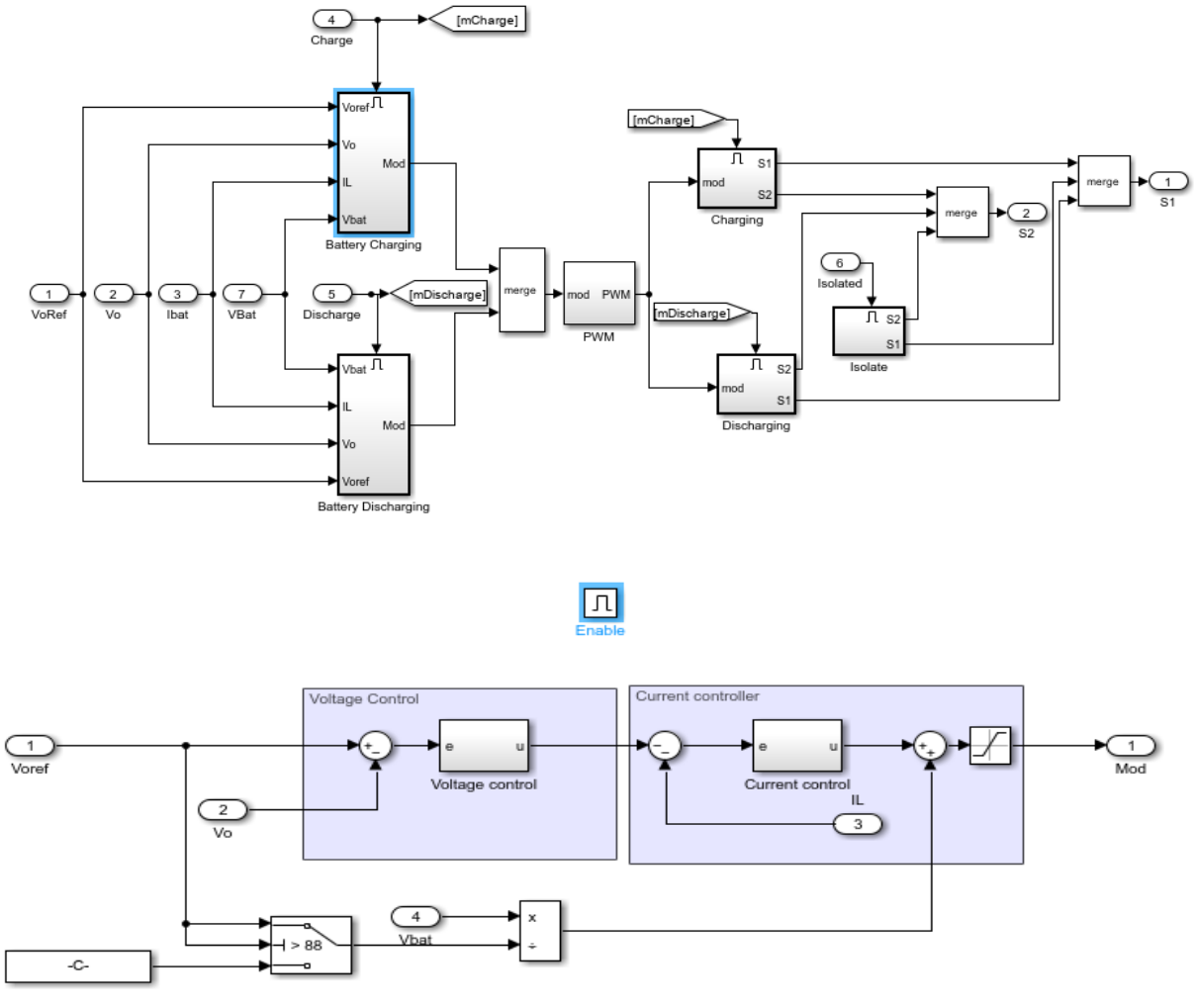

Figure 3. 16 Simulink Model of Battery Management

3.4.6 Control Strategy

The PV system's model includes seven operational modes. These modes are chosen based on the DC bus voltage, the PV array's output power, and the battery's charge state. The level of the DC bus voltage is utilized to identify any imbalance in the load. If the DC bus voltage exceeds the maximum VDC, it indicates that the system is producing more power than the load needs. Conversely, if the DC bus voltage falls below the minimum VDC, it means the load is demanding more power than the system can produce.

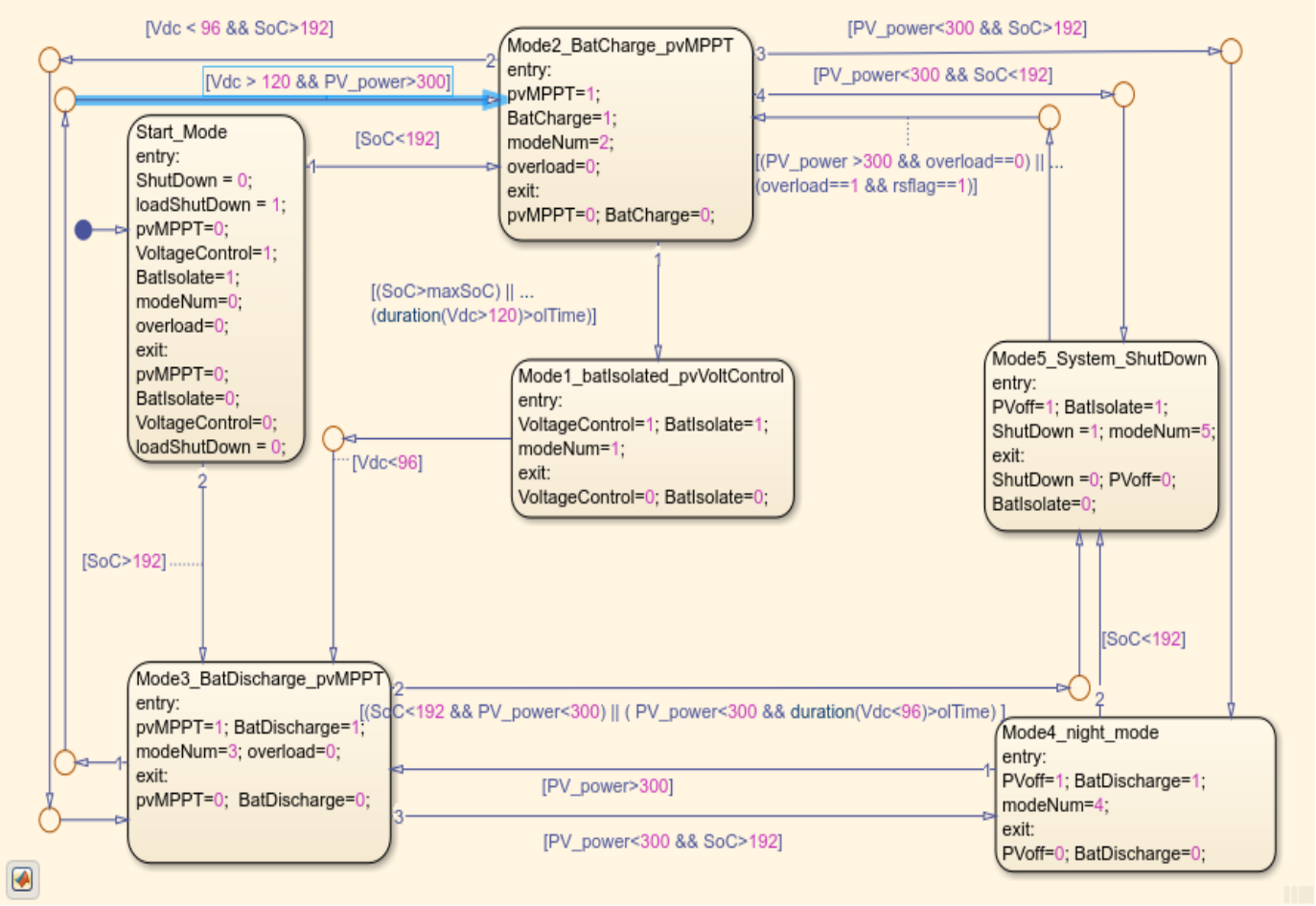

Figure 3. 17 Operation Mode Controller

Each operating mode of the modeled PV DC System is explained below

Mode-0 - Start mode

This mode is the default simulation starting mode. During the initial stage of the operation the buck convertor is connected to the 600VDC power supply of the locomotive, multistage voltage control circuit is turned ON to maintain the buck convertor's output to 110VDC, the loads and the battery will not be connected to the power system. After maintaining 110VDC the next operating mode will be selected depending on the state of charge of the battery. If the SoC is less than the minimum SoC, then the system will be operating in Mode-2 and if the SoC is greater than the minimum SoC, then the system will be operating in Mode-3.

Mode-1 - PV in output voltage control, battery fully charged and isolated.

The system operates in this mode when the battery is fully charged and the PV system can produce more power than required using MPPT. During the operation of this mode, the multi-stage voltage controller controls the output voltage to be 110VDC and the current to be as required by the DC load. Since the battery is fully charged and the PV system can alone supply the DC loads, the battery will be isolated till the load voltage is less than the minimum DC voltage. If the load voltage is less than the minimum DC voltage then this implies the PV is not able to supply the DC load by itself alone. Therefore, if the voltage drops less than the minimum DC voltage the system operation mode will be changed to Mode-3.

Mode-2 - PV in maximum power point, the battery is charging

The system operates in this mode when the PV system is generating more than required by the DC loads and when the battery is not fully charged. During the operation of this mode, the system enables the MPPT and charge controller to extract available maximum power to supply the loads and to charge the battery respectively. If the SoC of the battery is more than the maximum SoC or the DC load Voltage continues to be greater than the maximum DC load voltage, then this implies that the battery is fully charged. During this situation, the system operation mode will be changed to Mode 1. On the other hand, if the SoC of the battery is more than the minimum SoC and the DC load Voltage is less than the minimum DC load voltage, then this implies that the PV system cannot supply the DC load by itself alone. Therefore, the system changes its mode to Mode-3 which enables the DC loads to be supplied from both the battery and the PV.

If the irradiance on the PV panel continues to decrease the output power of the PV sub-system continues to drop down to less than the minimum PV power. During this condition, if the SoC is more than the minimum SoC, the operation mode will be changed to Mode-4 so that the battery will supply the loads. However, if the SoC is less than the minimum SoC then the system will change its operation mode to Mode 5. This implies the main supply from the locomotive will overtake the supply of the loads and battery.

Mode-3 - PV in maximum power point, the battery is discharging.

The system operates in this mode when the PV system is generating less than required by the DC loads and when the battery is in position to help serve the DC loads. During the operation of this mode, the system enables the MPPT and discharge controller to extract available maximum power and control the discharge of the battery so that they can provide the required power to the DC loads. If the DC load Voltage becomes greater than the maximum DC load voltage and the PV produces more power than the minimum PV power, then this implies that the PV system is producing more power than required by the DC loads. During this situation, the system operation mode will be changed to Mode 2. On the other hand, if the SoC of the battery is more than the minimum SoC and the PV is producing power is less than the minimum PV power, then this implies that the PV panels are receiving low irradiance. Therefore, to protect the PV array, the system changes its mode of operation to Mode-4 which enables the DC loads to be supplied only by the battery.

If the SoC of the battery continues to decrease and become the lower than minimum SoC, while the PV power generated is less than the minimum threshold then this implies that both the PV sub-system and the battery together cannot provide the demand of the load. In this situation, the system will change its operation mode to Mode 5 so that, the 600VDC main power supply from the locomotive takes over the supply of the load and battery.

Mode-4 - Night mode, PV shutdown, battery is discharging.

The system operates in this mode when the PV system is producing power less than the minimum PV power due to lower irradiance on the PV array. During this operation mode, the system enables the discharge controller and shutdown PV subsystem to supply DC loads only by

the battery. The PV subsystem is shut down to protect the PV array from working on low irradiance which reduces the array's lifetime.

If the PV subsystem produces power greater than the minimum power, then this implies the PV array is getting more irradiance so that it can supply the loads at least with the battery. Therefore, the operation mode will be changed to Mode 3.

Mode-5 – Main power supply (Night mode).

The system operates in this mode when the both PV subsystem and battery together cannot supply the demand of the DC loads. This situation may occur when the trains operate for the whole night only. During this operation mode, the 600VDC supply will be connected, the PV subsystem will be disconnected using change over circuit breaker. So that the DC load and the battery can be supplied from the main power supply system of the locomotive.

3.5 Economic Evaluation of the Designed System

To evaluate the feasibility of a photovoltaic system, it is imperative to ascertain the expenses associated with the implementation of the proposed PV system. Therefore, it is necessary to determine the cost of equipment involved, the installation cost, and the tariff of electricity.

Various direct methods can be employed to evaluate the profitability of a project. One straightforward economic indicator is the payback period, which calculates the time it takes for an investment to recoup its initial costs and is used to gauge the viability of an investment opportunity. It is defined as in Eq.3.16.

$$\text{Payback period} = \frac{\text{Total cost}}{(tariff * total\ energy)} \tag{3.16}$$

$$\text{ROI} = \frac{Profit}{Investment} \tag{3.17}$$

The initial cost of the system involves the PV panel cost, the MPPT charger cost, the cost of supporting structure of the PV panel, the wiring, and the breaker cost. The cost of a DSM370(Q) monocrystalline module is 0.165$/Wp, this means one (370W) panel is $61.05. On a single couch, 18 PV panels are going to be installed. For all the 60-passenger couches that EDR

planned to have, 1080 panels are required. Therefore, the total PV panel cost will be $65,934. The cost of an MPPT charger is $85.4 [73] for all the 60-passenger couches, 60 MPPT chargers are required. Therefore, the total MPPT charger cost will be $5,124. The PV panes needs to be connected and fixed on the train roofs, so the initial cost must include cost of a supporting structure, conductor and installation cost. Which is totally $1950. Therefore, the total initial investment cost becomes $73,008.

CHAPTER FOUR

RESULT AND DISCUSSION

This chapter presents a detailed analysis and discussion of the results obtained by following the methodology stated in the previous chapters.

4.1 Simulation Results

4.1.1 MPPT

As stated in the design section of this research, totally the 60 EDR passenger couches roof has 3000 m^2 available area for PV panel installation, on the available area by installing 1,080 DSM370(Q) PV panels maximum of 399.6 kW power can be harvested. For the simulation purpose, a single passenger couch is considered since all the PV systems designed for each of the 60 couches are similar.

Depending on the amount of irradiance collected by the PV panels, the maximum power output that can be harvested from a PV panel on a single couch is calculated to be 6.66kW.

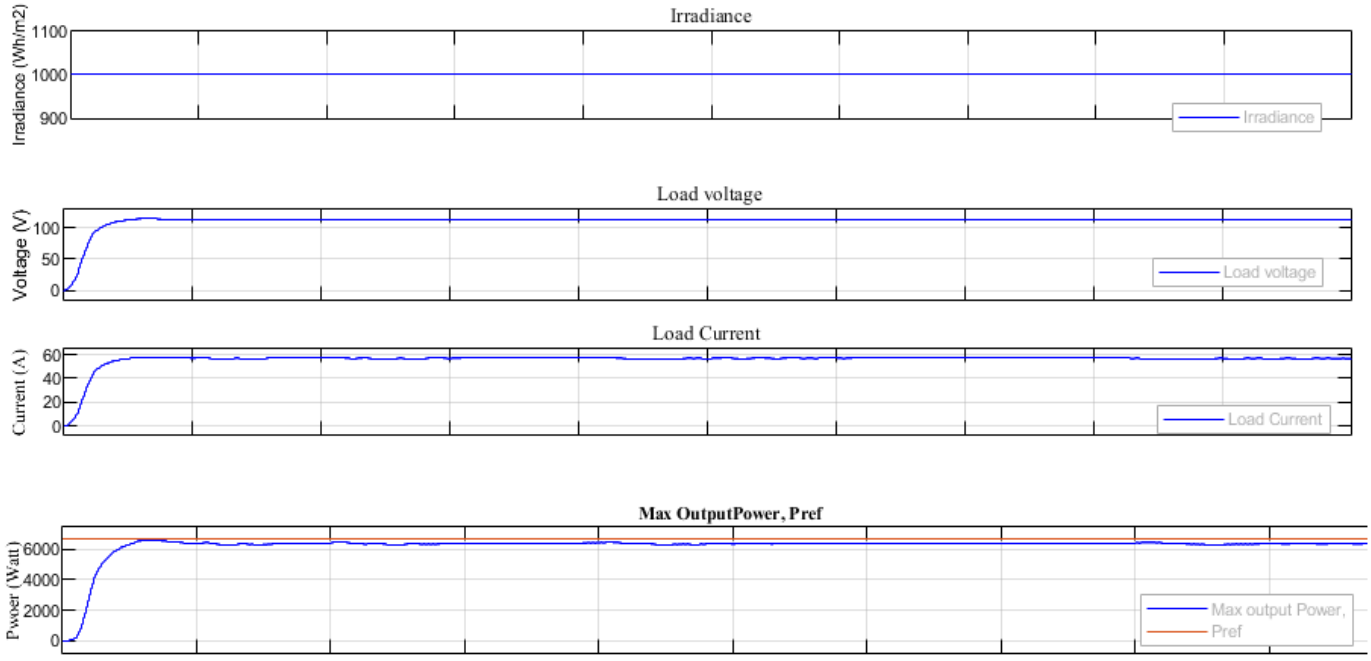

Figure 4. 1 The Simulation Result of the MPPT

The output of the simulation shows the output power has reached nearly the anticipated maximum power of 6.56 kW. The MPPT was able to track the maximum power with efficiency up to 98.4%.

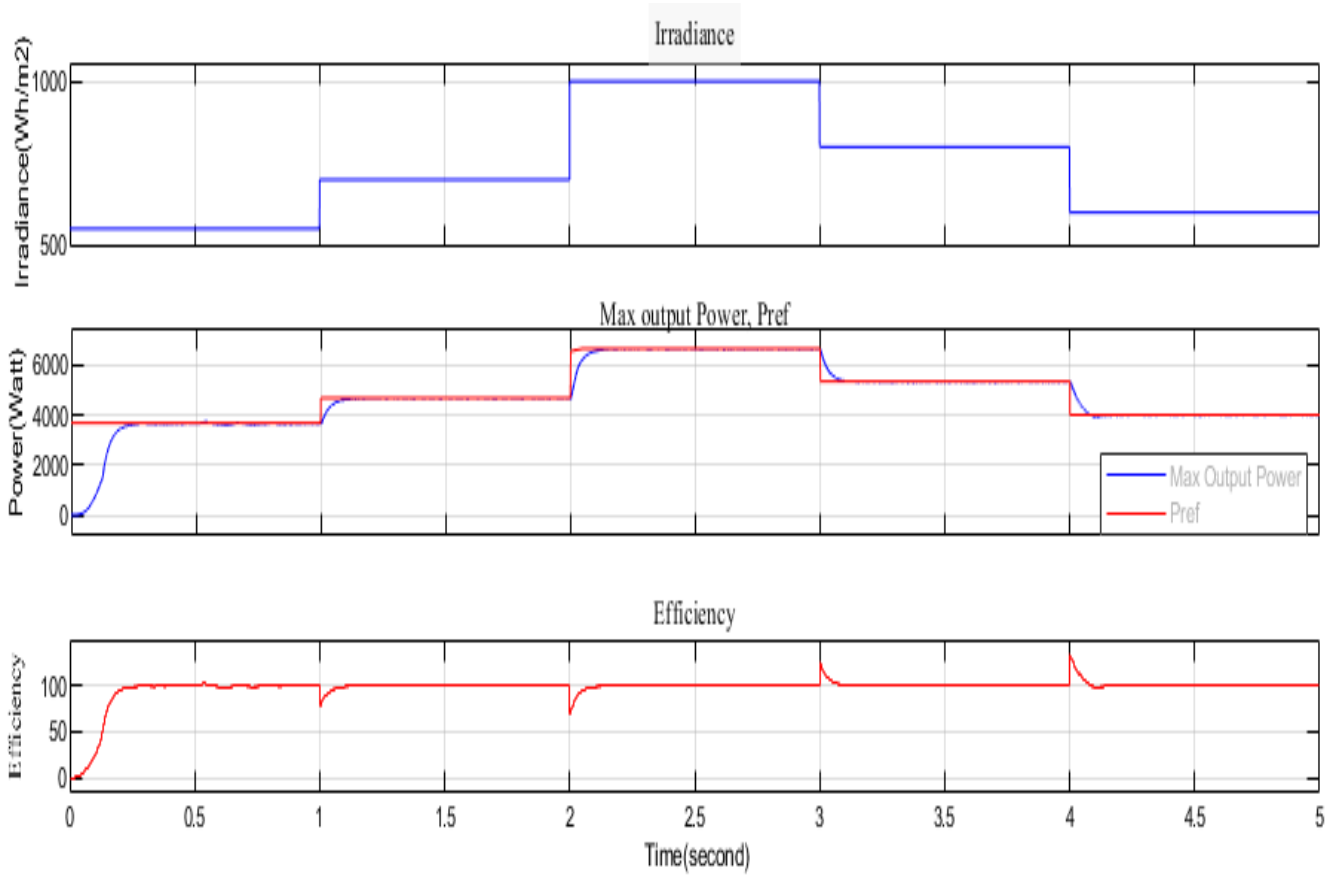

Figure 4. 2 The Simulation Result of the MPPT for Different Irradiance Values.

The result in Figure 4.2 shows that the MPPT can track the maximum power for varying irradiance. The tracking efficiency of the MPPT is of the MPPT is higher for higher irradiance compared to smaller irradiance. During the simulation at the 3-second and 4-second marks, the system's efficiency slightly exceeds 100%. This is attributed to the energy stored in the inductor and capacitor.

4.1.2 Battery Management System

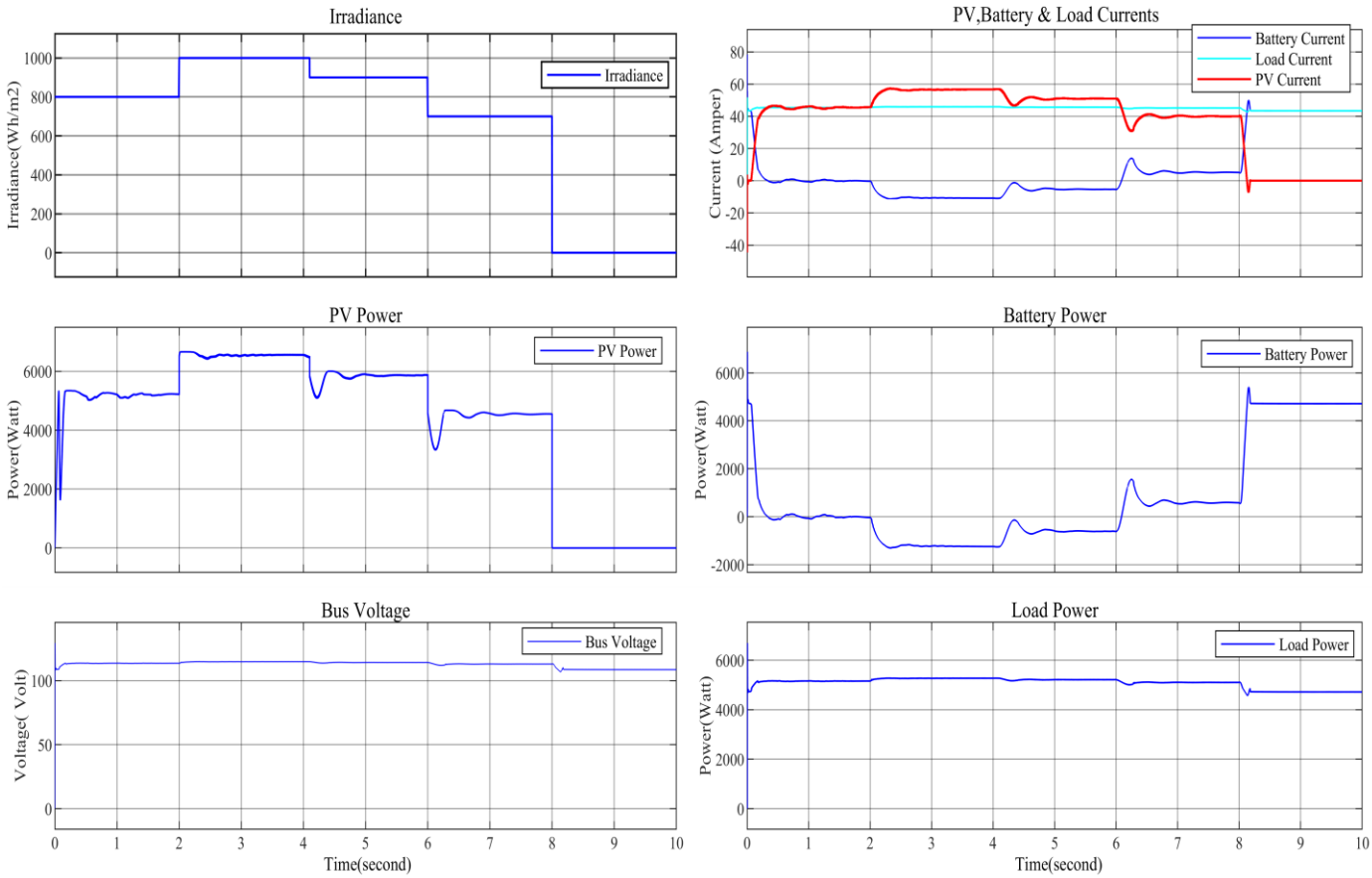

Figure 4. 3 Simulation Results of Battery Management System for Different Irradiance

The simulation results show that, for the first two seconds the irradiance is higher so as the power generated from the PV system, during this time the PV output power can supply the loads only by itself. For the next two seconds of the simulation, the irradiance is further increased, during this time the PV system not only supplies the load but also charges the battery. The battery current is negative and higher in magnitude. Between the simulation time of 4.05sec and 6sec the irradiance is reduced from 1000Wh/m^2 to 900Wh/m^2 during this time the charging is reduced but still, the PV system is supplying the loads and charging the battery. For the simulation time between 6sec and 8sec, the irradiance is further reduced to 700Wh/m^2, during this time the loads are served by both the PV system and the battery. The final two seconds of the simulation show that there is no sunlight therefore all the loads are served by the batteries only.

Generally, this simulation shows that for higher irradiance the voltage at the bus-bar tends to increase. Once the voltage hits its peak, the charging process of the battery commences. On the other hand, when the irradiance is reduced the power from the PV system will also be reduced and during this time the battery starts discharging to supply the DC loads. Therefore, the bus-bar voltage remains 110V DC and power to the load remains the same as long as the connected load is the same and the battery or the PV system can supply the loads. The result also showed that the maximum discharging and charging current of the battery is not exceeded.

4.2 Energy Demand-Supply Analysis of the Roof Top PV System

For Lebu- Diredawa and Diredawa - Lebu routes, a train that departs from one of the departure locations will return to its departure location the next day. Therefore, the average energy produced becomes 36.04kWh/day by a single couch for Lebu- Diredawa and Diredawa - Lebu routes. Among the produced energy by the PV system, 1.57kWh/day energy is used for propulsion of the additional weight, due to the PV panels, by the traction system. This implies on average more than 1.47kWh per day of extra energy is produced since the energy consumption for a single couch is 33kWh/day. However, there are cloudy and rainy days in a year when the PV system generates less than the energy required by the DC loads. For such a case, the energy stored in batteries from the previous day's charging will supply the load and in the worst-case scenario, the main supply system will supply the loads. The minimum and maximum daily energy productions are 24.2Wh/day and 45.16kWh/day respectively for the two routes.

The average energy produced by a train that travels between Diredawa and Negad is 40.82kWh/day, among the produced energy by the PV system, 1.98kWh/day by a single couch energy is used for propulsion of the additional weight, due to the PV panels, by the traction system. This implies the average energy production of a PV on a train that departs at 7:00 from Diredawa to Negad and back to Diredawa will serve the energy demand of the DC auxiliary loads only, whereas PV on a train that departs at 7:00 from Negad to Diredawa and back to Negad will produce on average more than 3kWh extra energy per day by the single couch since the energy consumption for a single couch is 2.8 kWh/day. However, there are cloudy and rainy days in a year when the PV system generates less than the energy required by the DC loads. For

such a case, the energy stored in batteries from the previous day's charging will supply the load and in the worst-case scenario, the main supply system will supply the loads. The minimum and maximum daily energy productions are 27.6kWh/day and 48.9kWh/day respectively for the travel.

4.3 Economic Analysis of Roof Top PV System

After assessing the energy production for departure time and locations. The economic analysis of the rooftop PV system, for those assessed departure times & locations, has been carried out using the payback period technique as indicated in Eq. 3.29. The initial investment cost for retrofitting the rooftop PV system is calculated to be 73,008USD which includes PV module cost, MPPT, power transmission cable cost, and configuration and installation costs. On the other hand, the electricity tariff of Ethiopian Electric Power for large industries is 0.654 Birr (0.012 USD) for each kWh of energy plus 43.82 Birr (0.8 USD) per month for the maximum power used during that month.

The total yearly energy production capacity of the rooftop PV system of the trains that depart from Lebu to Diredawa at 8:00, and from Diredawa to Lebu at 8:00 is 554.34 MWh per year, and among the capacity the total yearly energy demand of the trains that travel between Lebu and Diredawa is 481.8MWh per year. For international travel, the total yearly energy production of a train that departs from Negad to Diredawa and back to Negad at 7:00 is 302.8 MWh per year from Diredawa to Negad and back to Negad at 7:00 is 268.6 MWh per year and among the capacity of the rooftop PV system the total yearly energy demand by the train is 262.8 MWh per year. Therefore, the total demand for DC auxiliary systems of the Ethio-Djibouti railway passenger trains becomes 744.6 MWh/year, and since the maximum demand of the auxiliary system of a single passenger train is 4.5kW, a total 270kW peak power is required.

According to the energy and power demand, 8,935.2 USD per year for energy usage and 2,592 USD per year for power peak reduction can be saved. Totally 11,527.2 USD per year can be saved, which means the rooftop PV system can return its investment within 6 years and 4 months.

The analysis of energy demand and supply in Section 3.2 indicates that the annual energy output from the photovoltaic (PV) system exceeds the demand. Instead of wasting this excess energy, it can be harnessed to power passengers' mobile devices through the extension of USB ports from 5 Volt supplies. Additionally, it can be used to power entertainment devices such as televisions. This can be achieved without significantly increasing the cost or weight of the train.

If we consider all the energy produced by the PV system is utilized for the whole life span (25 years) of the PV panels, the rooftop PV system can contribute up to 21.318GWh of electric power to EDR passenger trains and yield a profit of 247,607 USD in its lifetime. Additionally, for this case, the ROI value of the PV system becomes 349%. The cash flow of each year of the PV panel lifetime is presented in Appendix VI.

CHAPTER FIVE
CONCLUSION AND RECOMMENDATION

5.1 Conclusion

The main purpose of this research was to design and model an efficient train rooftop photovoltaic system for Ethio-Djibouti passenger trains, that can supply DC auxiliary loads of the passenger trains. This was achieved through detailed designs and simulations considering the effect of the movement of the passenger train, unlike other conventional methods used for stationary PV systems.

The effective available area on the rooftop of EDR passenger couches and the angle of incidence for different times and locations during travel were calculated. Then the solar irradiance function of the train travel schedule across the train route is collected from the European Union weather forecasting web. The result showed that there is huge potential for solar energy. It also showed the energy production of the rooftop PV system varies for different departure times and locations.

After assessing the potential of solar energy, the energy demand of the train's auxiliary devices was assessed to balance supply and demand energy. Depending on the capacity of the PV system the load that can be served by the system is selected to be devices that are powered by the 8kW charger convertor. After selecting the load, the designed system is modeled and simulated using MATLAB. Furthermore, the effect of the PV system on the reliability of auxiliary devices was assessed. Finally, the feasibility of the system was studied.

The results of the simulation show that the MPPT tracks the maximum power point up to an efficiency of 98.4% and the battery and PV control system keeps the bus voltage 110VDC efficiently for different irradiance values. According to the analysis of energy supply and demand, combining the annual energy output of PV systems with battery energy can meet the annual energy needs of DC auxiliary loads. It has also been proven that the proposed PV system will contribute up to 21.318GWh of electric power to EDR passenger trains and yield a profit of 251,383 USD in its lifetime. Additionally, if the energy produced by the PV system is fully

utilized the ROI value and the payback period of the PV system become 349% and 6 years and 3 months respectively.

In conclusion, this research has successfully evaluated the viability of a train rooftop PV system as a power source for EDR passenger couches auxiliary devices using a unique approach. It has also designed and modeled an effective train rooftop PV system with energy storage specifically tailored for Ethio-Djibouti passenger trains. The findings indicate that the energy production of the PV system is influenced by the train's departure time and location. Moreover, the EDR passenger rooftop PV system possesses the capacity to generate ample energy to fulfill the DC auxiliary loads of the train. Implementing the train rooftop PV system results in reduced energy costs and enhanced reliability of power supply for vital equipment such as communication devices, safety mechanisms, and passenger comfort amenities like signaling devices, anti-skidding devices, and lighting devices.

5.2 Recommendation

Based on the increasing demand for electric power in the electric traction industry and the growing application of renewable energy sources like PV, this research aims to assess the potential of solar power for the Ethio-Djibouti railway route using a unique method. The findings indicate that rooftop PV systems have the potential to supply DC auxiliary loads for passenger trains. Consequently, it is recommended that EDR consider implementing PV power, which not only reduces energy costs but also improves the reliability of the 110V DC power system. Additionally, the potential assessment method employed serves as a valuable reference for future research efforts in this field. The specific measures proposed in this study to meet the DC auxiliary load requirements of passenger couches can offer significant practicality, particularly for other countries blessed with abundant solar energy resources.

Future research in this field is suggested to focus on four main areas. Firstly, the accuracy of energy production estimation can be significantly enhanced by increasing the resolution of irradiance data to 15-minute intervals or less. This would provide a more detailed understanding of irradiance variations, thereby enabling more precise energy production predictions.

Secondly, although the Maximum Power Point Tracking (MPPT) currently used is capable of collecting maximum power, there is potential for enhancing the efficiency of the system. This could be achieved by exploring and implementing more efficient hybrid MPPT algorithms. These advanced algorithms could optimize the power collection process, leading to an increase in the overall efficiency of the energy production system.

Lastly, the application of Photovoltaic systems for railway traction systems and AC auxiliary loads could be explored. The integration of renewable energy sources, such as PV systems, into railway traction could contribute to the sustainability and efficiency of railway operations.

These proposed directions for future research greatly enhance the progress of energy production technologies and the broader goal of achieving sustainable and efficient energy systems.

References

[1] B. Morris, F. Federica, and Z. Dario, “Introduction to Railway Systems,” in *Electrical Railway Transportation Systems*, John Wiley & Sons, Ltd, 2018, pp. 1–16. doi: https://doi.org/10.1002/9781119386827.ch1.

[2] X. Dong, “High-speed railway and urban sectoral employment in China,” *Transp Res Part A Policy Pract*, vol. 116, pp. 603–621, Oct. 2018, doi: 10.1016/J.TRA.2018.07.010.

[3] A. González-Gil, R. Palacin, and P. Batty, “Sustainable urban rail systems: Strategies and technologies for optimal management of regenerative braking energy,” *Energy Convers Manag*, vol. 75, pp. 374–388, Nov. 2013, doi: 10.1016/J.ENCONMAN.2013.06.039.

[4] M. Tilahun, “Study on Technical Feasibility and Design of Grid Connected Solar PV Based Power Supply System for The Ethio-Djibouti Railway Line,” MSc Thesis, Addis Ababa University, Addis Ababa, 2020.

[5] N. George and S. P. D. Chowdhury, “Roof-Top Solar Power Augmentation to Auxiliary Supply of Passenger Train,” *2018 IEEE PES/IAS PowerAfrica*, pp. 793–798, 2018, [Online]. Available: https://api.semanticscholar.org/CorpusID:53214452

[6] G. Schwerhoff and M. Sy, “Renewable energy sources, especially solar, are ideal for meeting Africa’s electrical power needs,” 2015. Accessed: Sep. 09, 2023. [Online]. Available: https://www.imf.org/en/Publications/fandd/issues/2020/03/powering-Africa-with-solar-energy-sy

[7] T. Mekonnen, R. Bhandari, and V. Ramayya, “Modeling, analysis and optimization of grid-integrated and islanded solar pv systems for the Ethiopian residential sector: Considering an emerging utility tariff plan for 2021 and beyond,” *Energies (Basel)*, vol. 14, no. 11, Jun. 2021, doi: 10.3390/en14113360.

[8] N. E. Benti, A. B. Aneseyee, A. A. Asfaw, C. A. Geffe, G. A. Tiruye, and Y. S. Mekonnen, “Estimation of global solar radiation using sunshine-based models in Ethiopia,” *Cogent Eng*, vol. 9, no. 1, 2022, doi: 10.1080/23311916.2022.2114200.

[9] Jameson Dow, “World’s First Solar-Powered train to begin operation in Australia,” Electrek. Accessed: Oct. 18, 2023. [Online]. Available: https://electrek.co/2017/12/14/worlds-first-solar-powered-train-to-begin-operation-in-australia/

[10] Khushboo Sandhu, “Himalayan Queen now fully solar powered,” The Indian Express. Accessed: Oct. 18, 2023. [Online]. Available: https://indianexpress.com/article/cities/chandigarh/himalayan-queen-now-fully-solar-powered/

[11] Ferenc Joo, “Solar-powered rail vehicle ready for service,” international railway journal. Accessed: Oct. 18, 2023. [Online]. Available: https://www.railjournal.com/rolling-stock/solar-powered-rail-vehicle-ready-for-service/

[12] R. Nibaruta, “Photovoltaic and Energy Storage Design for Auxiliary Loads of Electric Light Weight Train: Case of Addis Ababa Light Rail Transit,” MSc Thesis, Addis Ababa University, Addis Ababa, 2021.

[13] S. Kebede, “Design of Hybrid Solar Energy System for The Application of Train Locomotive Power Source for The AALRT And Ethio-Djibouti Routs,” MSc Thesis, Addis Ababa university, Addis Ababa, 2015.

[14] A. Belay *et al.*, “Comprehensive review and performance evaluation of maximum power point tracking algorithms for photovoltaic system,” *Global Energy Interconnection*, vol. 3, pp. 398–412, 2020, doi: 10.14171/j.2096-5117.gei.2020.04.010.

[15] O. Matsiko, “Optimal Method of Generating Power at the Train Rooftop for the Auxiliary Power Supply System Case Study: Solar and Wind Power Generation on Electric Multiple Units (EMU) at Addis Ababa Light Rail Transit System (AALRT),” MSc Thesis, Addis Ababa University, Addis Ababa, 2019.

[16] Anna Lina Ruscelli, Gabriele Cecchetti, Piero Castoldi Scuola Superiore, and S. Anna, “Energy harvesting for on-board railway systems,” in *5th IEEE International Conference*

on Models and Technologies for Intelligent Transportation Systems: proceedings: Napoli, Hotel Royal Continental, Jun. 2017, pp. 26–28.

[17] Huaxia, "Ethiopia-Djibouti railway transports 530,900 passengers," Xinhua. Accessed: Oct. 17, 2023. [Online]. Available: https://english.news.cn/20230703/2fe338622532451199214 0e24bbd653a/c.html

[18] C. Jeyaseelan, A. Jain, P. Khurana, D. Kumar, and S. Thatai, "Ni-Cd Batteries," in *Rechargeable Batteries*, John Wiley & Sons, Ltd, 2020, pp. 177–194. doi: https://doi.org/10.1002/9781119714774.ch9.

[19] Z. Huang and G. Du, "Nickel-based batteries for medium- and large-scale energy storage," in *Advances in Batteries for Medium and Large-Scale Energy Storage: Types and Applications*, Elsevier, 2015, pp. 73–90. doi: 10.1016/B978-1-78242-013-2.00004-2.

[20] J. Teng, L. Li, Y. Jiang, and R. Shi, "A Review of Clean Energy Exploitation for Railway Transportation Systems and Its Enlightenment to China," *Sustainability (Switzerland)*, vol. 14, no. 17. MDPI, Sep. 01, 2022. doi: 10.3390/su141710740.

[21] A. Dheyaa and A. Al-Nabooee, "The Economic and Environmental Feasibility of Using Renewable Energy in Public Transport: An Extensive Study," *African Journal of Advanced Pure and Applied Sciences (AJAPAS)*, vol. 1, no. 3, pp. 81–90, 2022.

[22] H. Kim, J. Ku, S. M. Kim, and H. D. Park, "A new GIS-based algorithm to estimate photovoltaic potential of solar train: Case study in Gyeongbu line, Korea," *Renew Energy*, vol. 190, pp. 713–729, May 2022, doi: 10.1016/j.renene.2022.03.130.

[23] F. Drake and Y. Mulugetta, "Assessment of solar and wind energy resources in Ethiopia. I. Solar energy," *Solar Energy*, vol. 57, no. 3, pp. 205–217, Sep. 1996, doi: 10.1016/S0038-092X(96)00094-1.

[24] N. Argaw, "ESTIMATION OF SOLAR RADIATION ENERGY OF ETHIOPIA FROM SUNSHINE DATA," *International Journal of Solar Energy*, vol. 18, pp. 103–113, 1996, [Online]. Available: https://api.semanticscholar.org/CorpusID:110074722

[25] F. T. Tekle, “Assessment of solar energy resources in Ethiopia: modeling solar radiation and GIS-based multi-criteria analysis,” 2014. [Online]. Available: https://api.semanticscholar.org/CorpusID:133908135

[26] Ethiopian resources group, *Diversity and Security for Ethiopian Power System: A Preliminary Assessment of Opportunities and Risks for the Power Sector*. Addis Ababa: Heinrich Böll Foundation, 2009. Accessed: Aug. 21, 2023. [Online]. Available: https://books.google.com.et/books/about/Diversity_and_Security_for_Ethiopian_Pow.html?id=tG_DYgEACAAJ&redir_esc=y

[27] F. Mark and John A. Dutton, “Utility Solar Power and Concentration,” e-Education Institute, College of Earth and Mineral Sciences, Penn State University. Accessed: Aug. 16, 2023. [Online]. Available: https://www.e-education.psu.edu/eme812/node/608

[28] S. A. Kalogirou, “Chapter nine - Photovoltaic Systems,” in *Solar Energy Engineering*, S. A. Kalogirou, Ed., Boston: Academic Press, 2009, pp. 469–519. doi: https://doi.org/10.1016/B978-0-12-374501-9.00009-1.

[29] T. Baines, T. P. Shalvey, and J. D. Major, “10 - CdTe Solar Cells,” in *A Comprehensive Guide to Solar Energy Systems*, T. M. Letcher and V. M. Fthenakis, Eds., Academic Press, 2018, pp. 215–232. doi: https://doi.org/10.1016/B978-0-12-811479-7.00010-5.

[30] E. Lorenzo and G. L. Araújo, “Solar Electricity: Engineering of Photovoltaic Systems,” 1994. [Online]. Available: https://api.semanticscholar.org/CorpusID:107771874

[31] S. Krauter, *Solar Electric Power Generation - Photovoltaic Energy Systems: Modeling of Optical and Thermal Performance, Electrical Yield, Energy Balance, Effect on Reduction of Greenhouse Gas Emissions*. Berlin: Springer Science & Business Media, 2006.

[32] M. Wei, W. Wei, H. Ruonan, and W. Ziyi, “Auxiliary power supply system of passenger train based on photovoltaic and energy storage,” in *2016 IEEE 11th Conference on Industrial Electronics and Applications (ICIEA)*, 2016, pp. 784–788. doi: 10.1109/ICIEA.2016.7603688.

[33] M. Shravanth Vasisht, G. A. Vashista, J. Srinivasan, and S. K. Ramasesha, “Rail coaches with rooftop solar photovoltaic systems: A feasibility study,” *Energy*, vol. 118, no. C, pp. 684–691, 2017, [Online]. Available: https://EconPapers.repec.org/RePEc:eee:energy:v:118:y:2017:i:c:p:684-691

[34] W. Yang and Z. Peng, “Comparative Analysis of the Reliability of Grid-Connected Photovoltaic Power Systems,” *IEEE PES general meeting; San Diego*, 2012.

[35] F. Dincer and M. E. Meral, “Critical Factors that Affecting Efficiency of Solar Cells,” *Smart Grid and Renewable Energy*, vol. 01, no. 01, pp. 47–50, 2010, doi: 10.4236/sgre.2010.11007.

[36] A. Pradhan and B. Panda, “Analysis of Ten External Factors Affecting the Performance of PV System,” in *International Conference on Energy, Communication, Data Analytics and Soft Computing*, Chennai, India, 2017, pp. 3093–3098. doi: 10.1109/ICECDS.2017.8390025.

[37] M. M. Fouad, L. A. Shihata, and E. S. I. Morgan, “An integrated review of factors influencing the performance of photovoltaic panels,” *Renewable and Sustainable Energy Reviews*, vol. 80. Elsevier Ltd, pp. 1499–1511, 2017. doi: 10.1016/j.rser.2017.05.141.

[38] A. Aslam, N. Ahmed, S. A. Qureshi, M. Assadi, and N. Ahmed, “Advances in Solar PV Systems; A Comprehensive Review of PV Performance, Influencing Factors, and Mitigation Techniques,” *Energies*, vol. 15, no. 20. MDPI, Oct. 01, 2022. doi: 10.3390/en15207595.

[39] M. Hosenuzzaman, N. A. Rahim, J. Selvaraj, and M. Hasanuzzaman, “Factors affecting the PV based power generation,” in *3rd IET International Conference on Clean Energy and Technology (CEAT) 2014*, 2014, pp. 1–6. doi: 10.1049/cp.2014.1467.

[40] J. D. Mondol, Y. G. Yohanis, and B. Norton, “The impact of array inclination and orientation on the performance of a grid-connected photovoltaic system,” *Renew Energy*, vol. 32, no. 1, pp. 118–140, 2007, doi: https://doi.org/10.1016/j.renene.2006.05.006.

[41] B. Wang *et al.*, “Research on influence between photovoltaic power and module temperature and ambient temperature,” in *2016 IEEE International Conference on Power System Technology (POWERCON)*, 2016, pp. 1–5. doi: 10.1109/POWERCON.2016.7753940.

[42] M. C. Alonso-García, J. M. Ruiz, and W. Herrmann, “Computer simulation of shading effects in photovoltaic arrays,” *Renew Energy*, vol. 31, no. 12, pp. 1986–1993, 2006, doi: https://doi.org/10.1016/j.renene.2005.09.030.

[43] C. Saiprakash, A. Mohapatra, B. Nayak, and S. R. Ghatak, “Analysis of partial shading effect on energy output of different solar PV array configurations,” *Mater Today Proc*, vol. 39, pp. 1905–1909, 2021, doi: https://doi.org/10.1016/j.matpr.2020.08.307.

[44] P. Dwivedi, K. Sudhakar, A. Soni, E. Solomin, and I. Kirpichnikova, “Advanced cooling techniques of P.V. modules: A state of art,” *Case Studies in Thermal Engineering*, vol. 21, 2020, doi: 10.1016/j.csite.2020.100674.

[45] A. A. Ashetehe, B. B. Gessesse, and F. Shewarega, “Development of Optimal Tilt Angle Models of a Photovoltaic Module for Maximum Power Production: Ethiopia,” *International Journal of Photoenergy*, vol. 2022, 2022, doi: 10.1155/2022/8729570.

[46] H. K. Elminir, A. E. Ghitas, F. El-Hussainy, R. Hamid, M. M. Beheary, and K. M. Abdel-Moneim, “Optimum solar flat-plate collector slope: Case study for Helwan, Egypt,” *Energy Convers Manag*, vol. 47, no. 5, pp. 624–637, 2006, doi: https://doi.org/10.1016/j.enconman.2005.05.015.

[47] A. A. Ashetehe, B. B. Gessesse, and F. Shewarega, “A generalized approach for the determination of optimum tilt angle for solar photovoltaic modules with selected locations in Ethiopia as illustration examples,” *Sci Afr*, vol. 18, p. e01433, 2022, doi: https://doi.org/10.1016/j.sciaf.2022.e01433.

[48] A. Al–bashir, M. Al-Dweri, A. Al–ghandoor, B. Hammad, and W. Al–kouz, “Analysis of effects of solar irradiance, cell temperature and wind speed on photovoltaic systems performance,” *International Journal of Energy Economics and Policy*, vol. 10, no. 1, pp. 353–359, 2020, doi: 10.32479/ijeep.8591.

[49] N. A. Kamarzaman and C. W. Tan, “A comprehensive review of maximum power point tracking algorithms for photovoltaic systems,” *Renewable and Sustainable Energy Reviews*, vol. 37. Elsevier Ltd, pp. 585–598, 2014. doi: 10.1016/j.rser.2014.05.045.

[50] H. Islam *et al.*, “Performance evaluation of maximum power point tracking approaches and photovoltaic systems,” *Energies (Basel)*, vol. 11, no. 2, Feb. 2018, doi: 10.3390/en11020365.

[51] K. A. Aganah and A. W. Leedy, “A constant voltage maximum power point tracking method for solar powered systems,” in *Proceedings of the Annual Southeastern Symposium on System Theory*, 2011, pp. 125–130. doi: 10.1109/SSST.2011.5753790.

[52] B. Bendib, H. Belmili, and F. Krim, “A survey of the most used MPPT methods: Conventional and advanced algorithms applied for photovoltaic systems,” *Renewable and Sustainable Energy Reviews*, vol. 45, pp. 637–648, 2015, doi: https://doi.org/10.1016/j.rser.2015.02.009.

[53] S. Khadidja, M. Mountassar, and B. M’hamed, “Comparative study of incremental conductance and perturb & observe MPPT methods for photovoltaic system,” in *2017 International Conference on Green Energy Conversion Systems (GECS)*, 2017, pp. 1–6. doi: 10.1109/GECS.2017.8066230.

[54] F. Çakmak, Z. Aydoğmuş, and M. R. Tür, “MPPT Control for PV Systems with Analytical Analysis Fractional Open Circuit Voltage Method,” in *2022 Global Energy Conference (GEC)*, 2022, pp. 130–135. doi: 10.1109/GEC55014.2022.9986746.

[55] M. Derbeli, C. Napole, and O. Barambones, “A Fuzzy Logic Control for Maximum Power Point Tracking Algorithm Validated in a Commercial PV System,” *Energies (Basel)*, vol. 16, no. 2, 2023, doi: 10.3390/en16020748.

[56] O. Ezinwanne, F. Zhongwen, and L. Zhijun, “Energy Performance and Cost Comparison of MPPT Techniques for Photovoltaics and other Applications,” in *Energy Procedia*, Elsevier Ltd, Feb. 2017, pp. 297–303. doi: 10.1016/j.egypro.2016.12.156.

[57] A. S. Shah, M. S. Ahmad, M. Noor, M. Qadeer, and A. Zaman, “A Comprehensive Review of Different Maximum Power Point Tracking Techniques,” *International Journal of Advanced Natural Sciences and Engineering Researches*, vol. 9, no. 9, pp. 193–199, 2023, [Online]. Available: https://as-proceeding.com/index.php/ijanser

[58] Asegid Belay, “Study the Potential Application of Renewable Energy System and Regenerative Braking in Traction System (Case study: Addis Ababa Light Rail Transit),” Ph.D. dissertation, Addis Ababa University, Addis Ababa, 2022.

[59] “JRC Photovoltaic Geographical Information System (PVGIS) - European Commission.” Accessed: Sep. 03, 2023. [Online]. Available: https://re.jrc.ec.europa.eu/pvg_tools/en/

[60] R. W. Mueller, C. Matsoukas, A. Gratzki, H. D. Behr, and R. Hollmann, “The CM-SAF operational scheme for the satellite-based retrieval of solar surface irradiance - A LUT based eigenvector hybrid approach,” *Remote Sens Environ*, vol. 113, no. 5, pp. 1012–1024, May 2009, doi: 10.1016/j.rse.2009.01.012.

[61] R. Mueller, T. Behrendt, A. Hammer, and A. Kemper, “A new algorithm for the satellite-based retrieval of solar surface irradiance in spectral bands,” *Remote Sens (Basel)*, vol. 4, no. 3, pp. 622–647, Mar. 2012, doi: 10.3390/rs4030622.

[62] T. Huld, R. Müller, and A. Gambardella, “A new solar radiation database for estimating PV performance in Europe and Africa,” *Solar Energy*, vol. 86, no. 6, pp. 1803–1815, Jun. 2012, doi: 10.1016/J.SOLENER.2012.03.006.

[63] H. Müllejans *et al.*, “State-of-the-art assessment of solar energy technologies Summary of the European Solar Test Installation’s contribution to the energy transition in 2020 and 2021.” Nov. 2022. doi: 10.2760/735053.

[64] Akshay Upadhyay, “Formula to Find Bearing or Heading angle between two points: Latitude Longitude.” Accessed: May 22, 2023. [Online]. Available: https://www.igismap.com/map-tool/bearing-angle

[65] Emebet Worku, “5G Radio Network Planning for Advanced Train to Ground Communication for Sebeta – Meiso Railway Line,” MSc Thesis, Addis Ababa, Addis Ababa, 2022.

[66] V. Benda, “Crystalline Silicon Solar Cell and Module Technology,” *A Comprehensive Guide to Solar Energy Systems*, pp. 181–213, Jan. 2018, doi: 10.1016/B978-0-12-811479-7.00009-9.

[67] Enfsolar, “Solar Trade Platform and Directory of Solar Companies Solar Panel Directory DSM370(Q).” Accessed: Oct. 09, 2023. [Online]. Available: https://www.enfsolar.com/pv/panel-datasheet/crystalline/58994?utm_source=ENF&utm_medium=panel_list&utm_campaign=enquiry_product_directory&utm_content=523

[68] V. Masterson, “Why don’t solar panels work as well in heatwaves?” Accessed: Aug. 09, 2023. [Online]. Available: https://www.weforum.org/agenda/2022/08/heatwaves-can-hamper-solar-panels/

[69] H. Goverde *et al.*, “Spatial and temporal analysis of wind effects on PV module temperature and performance,” *Sustainable Energy Technologies and Assessments*, vol. 11, pp. 36–41, 2015, doi: https://doi.org/10.1016/j.seta.2015.05.003.

[70] “How HOMER calculates the PV Array power Output.” Accessed: Aug 20,2023 [Online] Available:https:www.homerenergy.com/products/pro/doc/3.11/homer_calculates_the_PV_array power_output.html

[71] H. A. Kazem, T. Khatib, and K. Sopian, “Sizing of a standalone photovoltaic/battery system at minimum cost for remote housing electrification in Sohar, Oman,” *Energy Build*, vol. 61, pp. 108–115, Jun. 2013, doi: 10.1016/J.ENBUILD.2013.02.011.

[72] M. H. Rashid, *Power electronics handbook: devices, circuits, and applications*, 2nd ed. Burlington, MA: Elsevier/Academic Press, 2007.

[73] Enfsolar, “Solar Trade Platform and Directory of Solar Companies Solar Panel Directory DSM370(Q).”Accessed: Jan 02,2024 [Online] Available: https://www.enfsolar.com/pv/charge-controller-datasheet/4122?utm_source=ENF&utm_medium=charge_controller_more_series&utm_campaign=enquiry_product_directory&utm_content=144449.

Appendix

Appendix I: Main electrical circuit diagram of EDR Passenger train

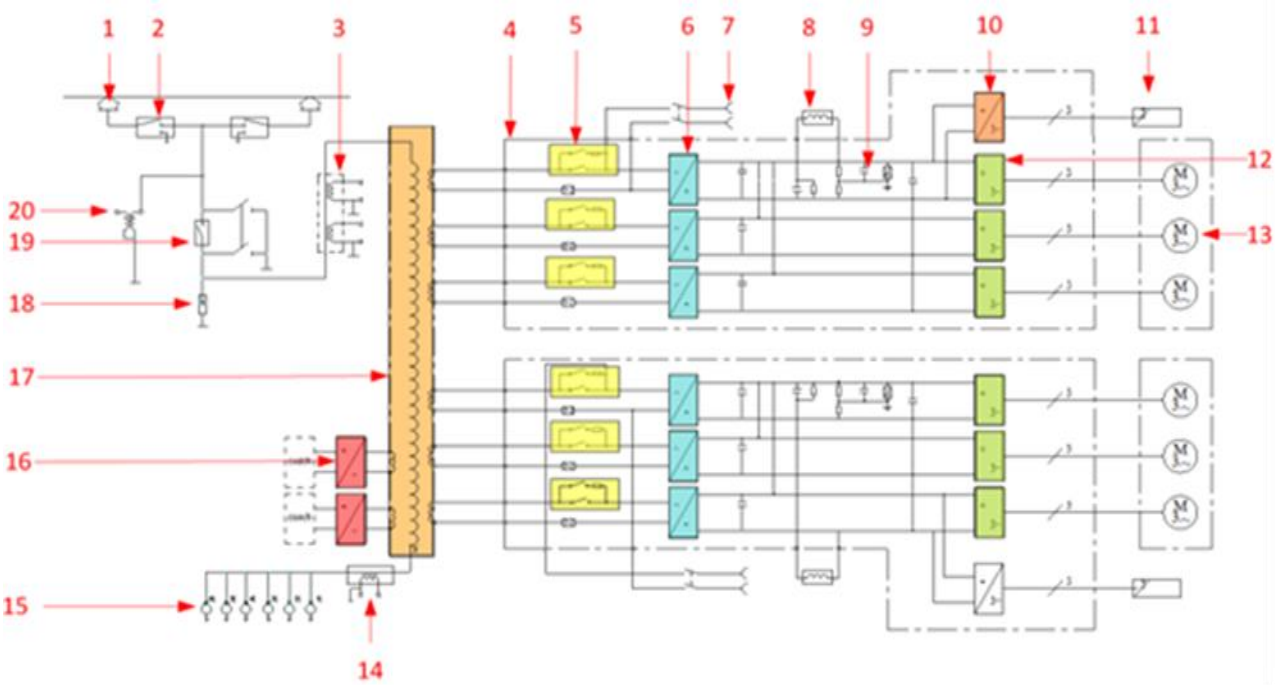

Main electrical circuit diagram of EDR passenger locomotive

No	Component	Function
1	Pantograph	Collect the 25kV power from contact network to the locomotive
2	High voltage isolator switch	Isolate fault pantograph
3	Primary current transformer	Detect primary current
4	Converter	Convert 25kV single-phase AC power into DC power and then Convert the DC power into three-phase AC power, which provides power for the traction motor
5	Pre-charging unit & line disconnector	Protect the electrical components in the converter when the locomotive starts
6	Four-quadrant converter	Convert AC power to DC power
7	Socket for driving in the shed	Move loco in the shed
8	Resonant circuit	Harmonic absorber
9	Bleeder resistor	Earth fault detection
10	Auxiliary inverter module	Supply auxiliary power
11	Auxiliary loads	Ensure the main circuit works normally

12	Traction PWM inverter module	Convert DC power to AC power
13	Traction motor	Supply loco traffic effort
14	Return current transformer	Detect return current
15	Earthing brush equipment	Lead the grounding current to the rail
16	Train power supply	Supply train power
17	Main transformer	Transform the 25kV power to lower power
18	Arrester	To protect the locomotive, avoid the impulse voltage from the contact line
19	High voltage breaker (HVB)	To cut the main circuit
20	High voltage transformer	Detect primary voltage

Appendix II: a) List of Power and Voltage Rating of a Single Passenger Couch Electrical Devices

Device name	Voltage rating	Rated power
Air conditioner	Three-phase AC 380V	40 kW
Water boiler	Three-phase AC 380V	4.5 kW
AC sockets	Single phase AC 220V	2 x 1.5 kW
Inverter controller	DC 110V	660 W
Battery Charger Controller	DC 110V	660 W
Water boiler controller	DC 110V	330 W
Evening and overnight lamps	DC 110V	1.5 kW
Bathroom lights	DC 110V	330 W
Emergency lights	DC 110V	660 W
Lighting control box	DC 110V	330 W
Deject collecting control devices	DC 110V	660 W
Broadcast power box, sound and light indicator, and axle temperature recorder	DC 110V	110 W
Toilet display	DC 110V	330 W
DY1 & DY2	DC 110V	200W
Anti-skid device	DC 48V	120W
PLC and HMI	DC 24V	35W

B) Summary of Lighting Fixtures For Passenger Vehicles

No	Lighting name	Wattage (rating)	Vehicle type & Qty.			
			HSC	HBC	SBC	DPC
1	Light ban	1x36W	28			35
2	Light ban	1x20W				1
3	Dome light	2x15W	6	7	17	6
4	Dome light	2x18W		22	9	
5	Wall lamp	1x15W	28	2	2	26
6	Wall lamp	2x15W	1			
7	Wall lamp	3x15W		1	1	
8	Spotlight					7
9	Reading light				4	
10	PA (public access)		4	4		2

The above quantity of lighting fixtures is for a single car/couch and

- HSC stands for Hard Seat Couch; it is a vehicle with a seating capacity of 118 persons.
- HBC stands for Hard Berth Couch; it is a vehicle with 66 sleeping beds.
- SBC stands for Soft Berth Couch; it is a vehicle with 36 sleeping beds.
- DPC stands for Dining passenger couch; used only for cafeteria and has 50 person seating capacity

Appendix III: DSM370(Q) I-V& P-V curve of 18 series module 1 parallel strings

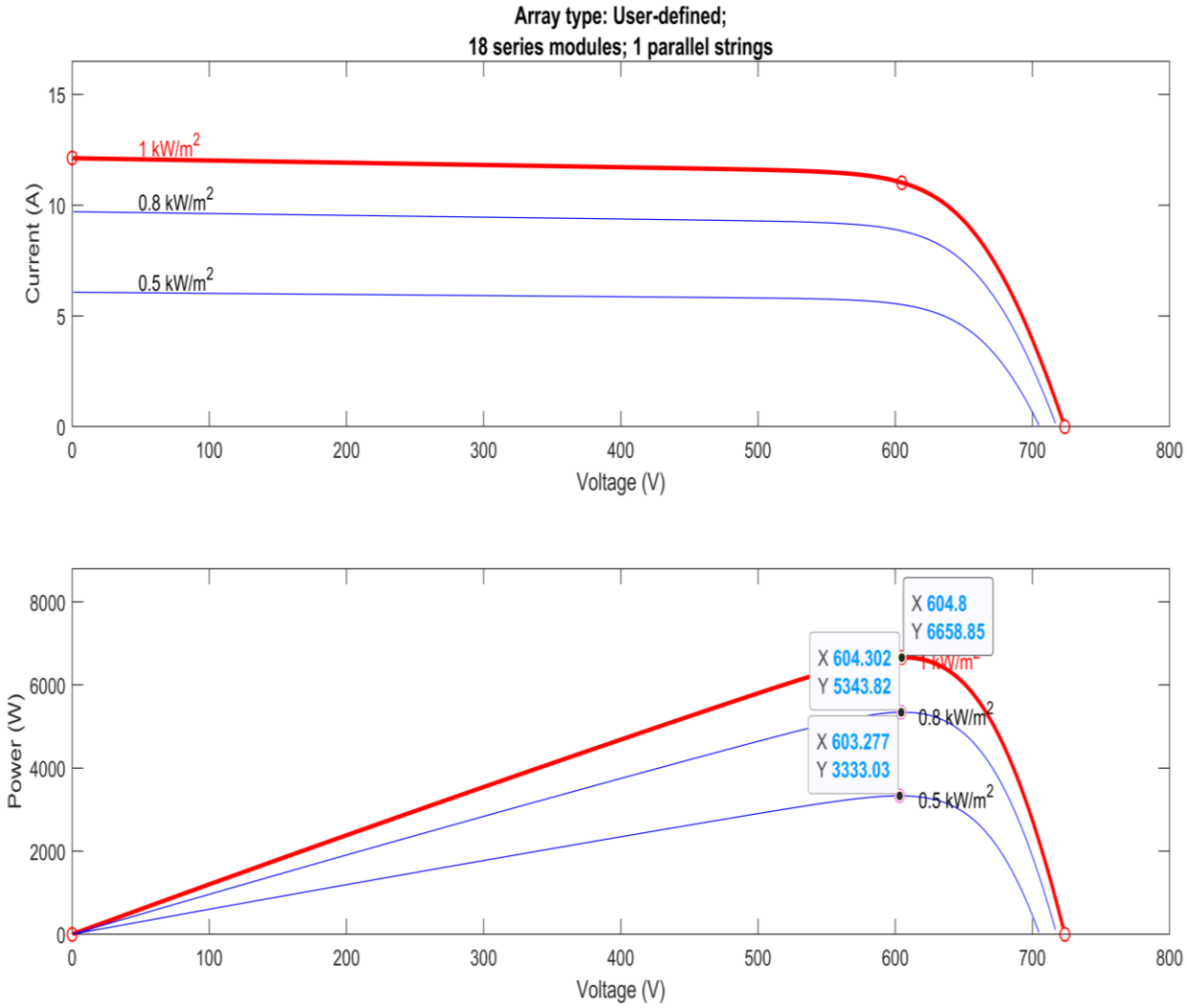

Appendix IV: Simulink Modele of Train Rooftop PV System.

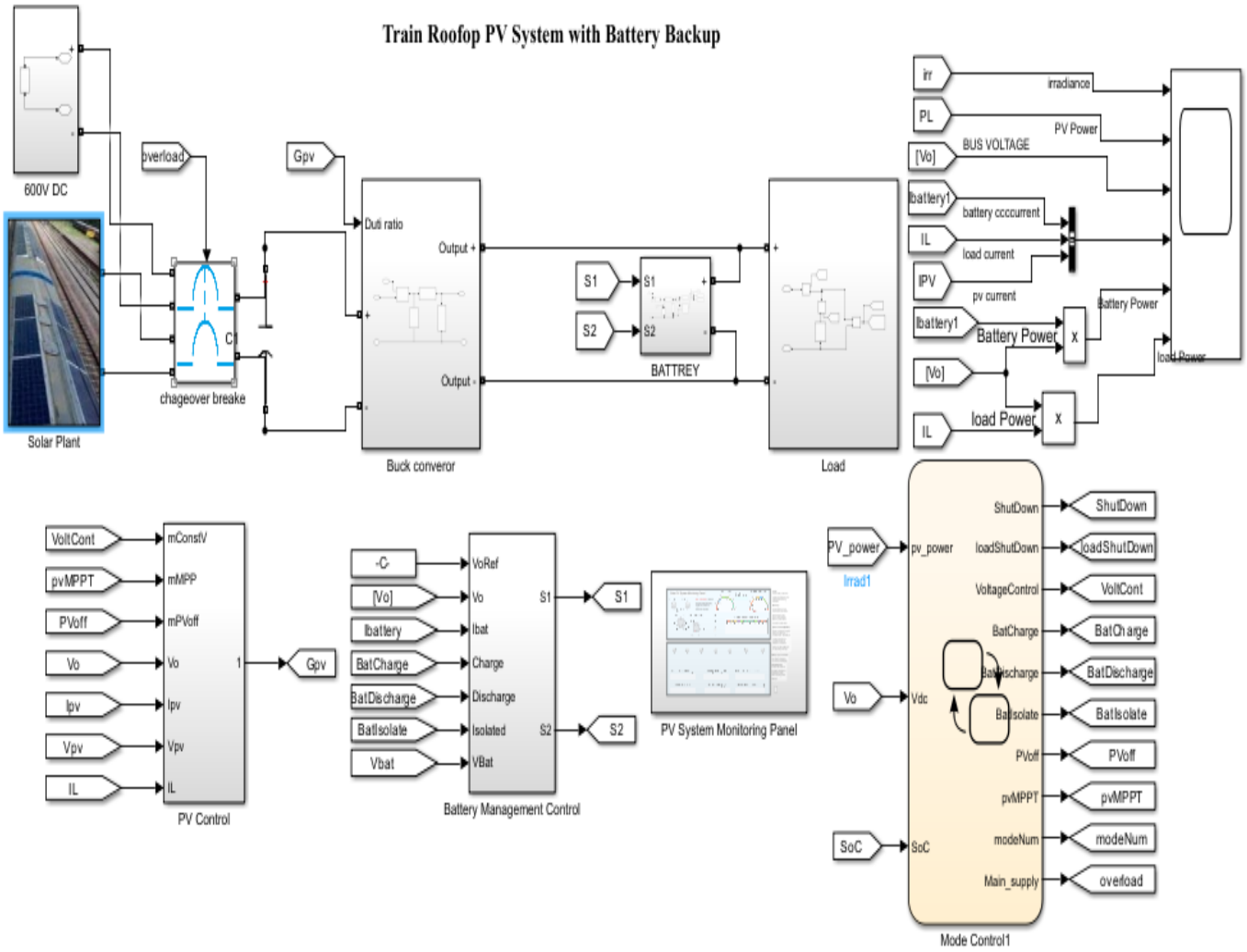

Appendix V: Cash Flow for the Roof Top PV System of EDR Passenger Couches

Year	Energy Production (MWh)	Cash Flow (in USD)	Cumulative Cash Flow (in USD)
0		-73,008	-73,008
1	915.43	13577.16	-59,431
2	909.97	13511.64	-45,919
3	904.54	13446.48	-32,473
4	899.15	13381.8	-19,091
5	893.79	13317.48	-5,773
6	888.46	13253.52	7,480
7	883.16	13189.92	20,670
8	877.89	13126.68	33,797
9	872.65	13063.8	46,860
10	867.45	13001.4	59,862
11	862.28	12939.36	72,801
12	857.14	12877.68	85,679
13	852	12816	98,495
14	846.89	12754.68	111,250
15	841.81	12693.72	123,943
16	836.76	12633.12	136,576
17	831.74	12572.88	149,149
18	826.75	12513	161,662
19	821.79	12453.48	174,116
20	816.86	12394.32	186,510
21	811.96	12335.52	198,846
22	807.09	12277.08	211,123
23	802.25	12219	223,342
24	797.44	12161.28	235,503
25	792.66	12103.92	247,607
	21317.91	247,607	247,607